

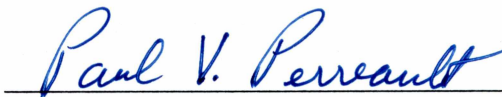
NUMERICAL ANALYSIS OF STRUCTURAL BEHAVIOR OF WELDED WIRE
REINFORCEMENT IN REINFORCED CONCRETE BEAMS

By


Radhakrishnan Balasubramanian
(ராதாகிருஷ்ணன் பாலசுப்ரமணியன்)

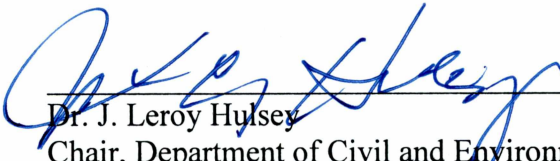
RECOMMENDED:


Dr. Chuen – Sen Lin

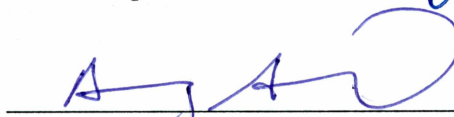

Mr. Paul V. Perreault

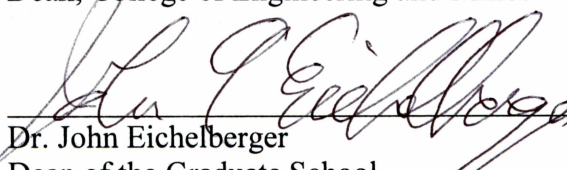

Dr. Il – Sang Ahn
Advisory Committee Co – Chair

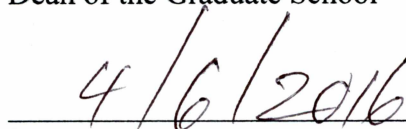

Dr. J. Leroy Hulsey
Advisory Committee Chair


Dr. J. Leroy Hulsey
Chair, Department of Civil and Environmental Engineering

APPROVED:


Dr. Douglas Goering
Dean, College of Engineering and Mines


Dr. John Eichelberger
Dean of the Graduate School


Date

NUMERICAL ANALYSIS OF STRUCTURAL BEHAVIOR OF WELDED WIRE
REINFORCEMENT IN REINFORCED CONCRETE BEAMS

A
THESIS

Presented to the Faculty
of the University of Alaska Fairbanks

in Partial Fulfillment of the Requirements
for the Degree of

MASTER OF SCIENCE

By

Radhakrishnan Balasubramanian, B.E.

(ராதாகிருஷ்ணன் பாலசுப்ரமணியன், பி.இ.,)

Fairbanks, AK

May 2016

Abstract

Modernization and industrialization have paved the way for the construction industry of India to expand. On the other hand the Indian construction industry is set to face an acute workforce shortage. The shortage of construction workers has in fact slowed down the growth of this industry in major cities across the country and escalated its cost by 40 percent. An alternative way to replace the labor force is by automation techniques.

This study is a numerical analysis to evaluate structural behavior of simply supported concrete beams reinforced with welded wires in comparison with mild steel reinforced concrete beams. Welding conventional steel bars (60 ksi) reduces their shear strength by 50 percent. Welded Wire Reinforcement (80 ksi), with its greater strength, higher durability, significantly lower placing and overall cost, provides an alternative and perhaps a better substitution for mild steel bars. The commercial finite element analysis program, ABAQUS, was used to model the non-linear behavior of reinforced concrete beams. In order to evaluate the structural behavior of welded wire reinforced concrete beams, different configurations of longitudinal and transverse wires have been considered.

First, different types of stirrup configurations in a rectangular reinforced concrete beam are compared with a conventional reinforced beam. Second, a structurally performing welded wire configuration is compared with a Mexican chair styled reinforcement configuration. This part of the analysis is evaluated for a T-beam, used for building roof applications.

Table of Contents

Signature Page	i
Title Page	iii
Abstract.....	v
Table of Contents.....	vii
List of Figures.....	xi
List of Tables	xv
Acknowledgements.....	xvii
Chapter 1 Introduction.....	1
1.1 Welded Wire Reinforcement	1
1.1.1 Traditional Rebar versus Welded Wire Reinforcement (WWR)	4
1.1.2 Potential Gains through Welded Wire Reinforcement (WWR).....	5
1.1.3 Welded Wire Reinforcement Specifications and Nomenclature.....	6
1.1.4 Welded Wire Reinforcement Manufacturing, Handling and Placing	10
1.2 Aim and Scope	13
1.3 Outline of Thesis.....	13
Chapter 2 Literature Review.....	15
2.1 Impact of Welded Wire Reinforcement in Structural Members.....	15
2.1.1 Welded Wire Reinforcements in Columns.....	15

2.1.2 Welded Wire Reinforcements in Beams and Girders	16
2.1.3 Welded Wire Reinforcements in Structural Walls	17
2.2 Summary	18
Chapter 3 Finite Element Modeling of Reinforced Concrete Beams	19
3.1 ABAQUS Modeling.....	19
3.2 Non-linear Behavior of Concrete	19
3.2.1 Uniaxial and Biaxial Behavior	19
3.3 Non-linear Modeling of Reinforced Concrete Beam	22
3.4 Material Model Properties	24
3.4.1 Concrete Damage Plasticity Parameters.....	24
3.4.2 Reinforcement Properties	27
3.5 Convergence Analysis.....	29
Chapter 4 Numerical Analysis of Concrete Beams Reinforced with Traditional and Welded Wire Reinforcement.....	31
4.1 Introduction	31
4.2 Initial Validation and Mesh Convergence	38
4.3 Analysis of Welded Wire Reinforcement Grids in Reinforced Concrete Beams ...	47
4.3.1 Rectangular Reinforced Concrete Beams Subjected to Four Point Loading Condition.....	47

4.3.2 Rectangular Reinforced Concrete Beams Subjected to Uniformly Distributed Loading Condition.....	56
4.3.3 T - Beams Subjected to Four Point Loading Condition	61
Chapter 5 Conclusion and Recommendation	67
5.1 Conclusion	67
5.2 Recommendation	68
References.....	71

List of Figures

Figure 1.1: Welded Wire Reinforcement for Concrete Girders.....	1
Figure 1.2: Uniformly Spaced Welded Wire Reinforcement	3
Figure 1.3: Differentially Spaced Welded Wire Reinforcement	4
Figure 1.4: Standard Laying Time for Traditional Rebar and Welded Wire Reinforcement	5
Figure 1.5: Cost Comparison for Traditional Rebar and Welded Wire Reinforcement	6
Figure 1.6: Longitudinal Wire Fed into Automated Welding Machine.....	11
Figure 1.7: Longitudinal and Transverse Wire Welding	11
Figure 1.8: Crane Handling of Welded Wire Reinforcement Bundle	12
Figure 1.9: Welded Wire Reinforcement Mesh Bending Machine	12
Figure 2.1: Welded Wire Column Reinforcement.....	16
Figure 2.2: Welded Wire Stirrup with Longitudinal Rebar	17
Figure 3.1: Uniaxial Compressive Behavior of Concrete.....	20
Figure 3.2: Yield Surface in Plane Stress	22
Figure 3.3: Hyperbolic Plastic Flow Rule.....	25
Figure 3.4: Conventional (60 ksi) and WWR (80 ksi) Steel Stress Strain Graph.....	28
Figure 4.1: Four Point Bending Test Setup	33
Figure 4.2: Cross Sectional Details of Beam B1RC	33
Figure 4.3: Cross Sectional Details of Beam B2WWR	34
Figure 4.4: Cross Sectional Details of Beam B3WWR	34
Figure 4.5: Cross Sectional Details of Beam B4WWR	35
Figure 4.6: Four Point Bending Test Setup of T - Beam	36
Figure 4.7: Cross Sectional Details of T- Beam TB1MS	36

Figure 4.8: Cross Sectional Details of T- Beam TB2WWR.....	37
Figure 4.9: Experimental Beam Cross Section.....	38
Figure 4.10 Four Point Bending Test Setup for Experimental Beam.....	38
Figure 4.11: Beam when Placed in the Test Setup.....	39
Figure 4.12: Experimental Beam Mesh Size 1 inch (25 mm).....	41
Figure 4.13: Experimental Beam Mesh Size 2 inch (50 mm).....	41
Figure 4.14: Experimental Beam Mesh Size 3 inch (75 mm).....	42
Figure 4.15: Load versus Deflection Graph for Experimental Beam.....	43
Figure 4.16: Reinforced Concrete Beam (B1RC) of 1 inch (25 mm) Mesh Size.....	44
Figure 4.17: Reinforced Concrete Beam (B1RC) of 2 inch (50 mm) Mesh Size.....	45
Figure 4.18: Reinforced Concrete Beam (B1RC) of 3 inch (75 mm) Mesh Size.....	45
Figure 4.19: Load versus Deflection Graph for Beam B1RC.....	47
Figure 4.20: Four Point Bending Test Setup.....	48
Figure 4.21: Open Leg Stirrup Embedded in B1RC Beam.....	48
Figure 4.22: Welded Wire Reinforced B2WWR Beam.....	49
Figure 4.23: Virtual Four Point Bend Test Setup for the Beam.....	49
Figure 4.24: Deformed Behavior of B4WWR Beam after Analysis.....	50
Figure 4.25: Load versus Deflection Graph for Rectangular Beams.....	51
Figure 4.26: B1RC Concrete and Steel Strain along Length of Beam.....	52
Figure 4.27: B2WWR Concrete and Steel Strain along Length of Beam.....	52
Figure 4.28: B3WWR Concrete and Steel Strain along Length of Beam.....	53
Figure 4.29: B4WWR Concrete and Steel Strain along Length of Beam.....	53
Figure 4.30: Uniformly Distributed Loaded Rectangular Beam.....	56

Figure 4.31: B1RC beam subjected to Uniformly Distributed Loading Condition.....	57
Figure 4.32: B1RC Concrete and Steel Strain along Length of Beam	57
Figure 4.33: B2WWR Concrete and Steel Strain along Length of Beam	58
Figure 4.34: B3WWR Concrete and Steel Strain along Length of Beam	58
Figure 4.35: B4WWR Concrete and Steel Strain along Length of Beam	59
Figure 4.36: Four Point Bend Test Setup for T – Beam	61
Figure 4.37: Mexican Chair Styled Reinforcement Embedded in T - Beam (TB1MS).....	62
Figure 4.38: Welded Wire Mesh Embedded in T - Beam (TB2WWR)	62
Figure 4.39: TB1RC beam subjected to Four Point Bend Test	63
Figure 4.40: Deflected Shape of TB2WWR after Analysis.....	63
Figure 4.41: TB1MS, TB2WWR Load versus Deflection Graph	64

List of Tables

Table 1.1: Welded Wire Reinforcement Item Description	8
Table 1.2: ASTM Specifications.....	9
Table 1.3: Weld Shear Strength for WWR.....	9
Table 3.1: Concrete Damage Plasticity Parameters.....	26
Table 3.2: Concrete Compressive Stress versus Strain.....	27
Table 4.1: B1RC, B2WWR, B3WWR, B4WWR Beam Properties	35
Table 4.2: TB1MS and TB2WWR Beam Properties.....	37
Table 4.3: Various Mesh size and Element Type for Experimental Beam.....	42
Table 4.4: Various Mesh size and Element Type for Beam B1RC	46
Table 4.5: Moment and Shear Capacity for Beams under Four Point Loading Condition.....	54
Table 4.6: Ductility Factor for Beams under Four Point Loading Condition.....	55
Table 4.7: Moment Capacity for Beams under Uniformly Distributed Loading Condition.....	60
Table 4.8: Moment and Shear Capacity for T-Beam Subjected to Four Point Bending Test.....	65

Acknowledgements

First of all, I thank my parents, Mr. Balasubramanian, Mrs. Rajathi Balasubramanian and my sister Sneha Balasubramanian, for their unconditional love and support to achieve my goals.

Special thanks to my principal advisor Dr. J. Leroy Hulsey for his constant support, encouragement and invaluable guidance during my graduate studies and in my career. I also greatly appreciate my advisory committee members Dr. Il – Sang Ahn, Dr. Chuen – Sen Lin and Paul V. Perreault for their valuable suggestions and commitment to this thesis.

Finally, I would like to thank my fellow students and friends, who helped me and made my time a memorable one which I will never forget in my life.

Chapter 1 Introduction

1.1 Welded Wire Reinforcement

Welded Wire Reinforcement (WWR) is a mesh of plain or deformed wire of high-strength welded together by an automatic welding machine in square or rectangular grids. As recognized by American Concrete Institute building code (ACI 318) and American Society for Testing and Materials (ASTM), the smaller diameter, closely-spaced wires of WWR provide more uniform stress distribution and effective crack control when compared to larger diameter bars. Concrete structures being successful and economically reinforced with WWR can be a greater benefit. Advantages can result in material savings, reduced construction time, and reduced overall project cost (Wire Reinforcement Institute 2006). Figure 1.1 shows a welded wire reinforced shear cage for concrete girders.



Figure 1.1: Welded Wire Reinforcement for Concrete Girders (Wire Reinforcement Institute 2006)

In 1901, John Perry from Massachusetts filed a patent for a machine that was able to weld wires in a sheet form, His initial idea was used to weld wire sheets for fences. In 1906, these welded wire sheets were used as reinforcement in concrete, and WWR got its first major application in the construction of the Long Island Parkway, New York in 1908. Since then WWR had a greater market in eastern states for usage in pavements. In 1922, a study took place on 78 different types of road pavement in Bates, Illinois. As a result, one of the engineers observed that WWR is the best fit for heavy traffic pavement. The result convinced a number of states to use WWR in their roads (Purdue 2015).

In 1956, President Eisenhower signed the National Highway Act and the states started building superhighways. Just prior to World War II, Pennsylvania started to work with WWR for highways between Irwin and Carlisle. Other states followed Pennsylvania's lead, and WWR was used for highways in Ohio, New York, Indiana, Oklahoma, and other states. For building construction, New York City offered a perfect platform for WWR in secondary structural components (floor slabs) because of the major fires that plagued the city. The city studied ways to improve fireproofing in buildings (Purdue 2015).

WWR has also been used for various projects like airport runways (O'Hare Airport, George W. Bush Airport), architecturally groundbreaking buildings (PanAm World Airways Terminal at JFK Airport and the Eli Lilly Plant in Indianapolis) and seating tiers for sports stadiums (Baltimore Ravens Stadium, Camden Yards and the Seattle Seahawks Stadium), because of its flexibility in offsite pre-cast geometric designs (Purdue 2015).

Structurally speaking, WWR played a significant role in the resilience of the Pacific Park Plaza Building during the Loma Prieta earthquake. In a report published by the Concrete Reinforcing Steel Institute in 1990, Dr. S. K. Ghosh said "The Pacific Park Plaza was

undamaged after experiencing significantly strong ground shaking” and WWR was used in all the beam and column joints as shear reinforcement in that building. By the close of World War II, WWR was the perfect alternative for reinforcing concrete structures in Europe. The success of the post-war rebuilding effort made European builders, architects, and engineers start to realize WWR’s potential. In fact, WWR is extremely popular in Europe, The United Arab Emirates and other countries because construction labor is expensive and builders are keen on keeping costs low and getting projects completed quicker (Purdue 2015). Uniform and non-uniform welded wire mesh spacing is shown in Figure 1.2 and Figure 1.3



Figure 1.2: Uniformly Spaced Welded Wire Reinforcement (Welded Wire Mesh 2012)



Figure 1.3: Differentially Spaced Welded Wire Reinforcement (Welded Wire Mesh 2012)

1.1.1 Traditional Rebar versus Welded Wire Reinforcement (WWR)

- i. Material fabrication is automated, which can save construction time, labor and material cost.
- ii. In extreme weather conditions, building construction can be accelerated.
- iii. The placement of reinforcement is usually in critical paths and employing WWR can save site space for rebar assembly.
- iv. A wide range of wire size and spacing allows flexibility in construction.
- v. The use of WWR reduces improper bending, misplacement and missing of bars since the process is automated.
- vi. Because the wires are welded they don't move when placed in concrete.

1.1.2 Potential Gains through Welded Wire Reinforcement (WWR)

For beam cages, use of WWR reduces installation time by half. As shown in Figure 1.4, for slab reinforcement, the productivity increase was 15 man hours per ton, and labor time savings was 4 to 11 times greater than normal (Arbeitszeitwerte 1977). Productivity of WWR for some flat slabs with two layers can be increased by 250%. Greater time savings occurred for columns and walls (Bernold and Chang 1992).

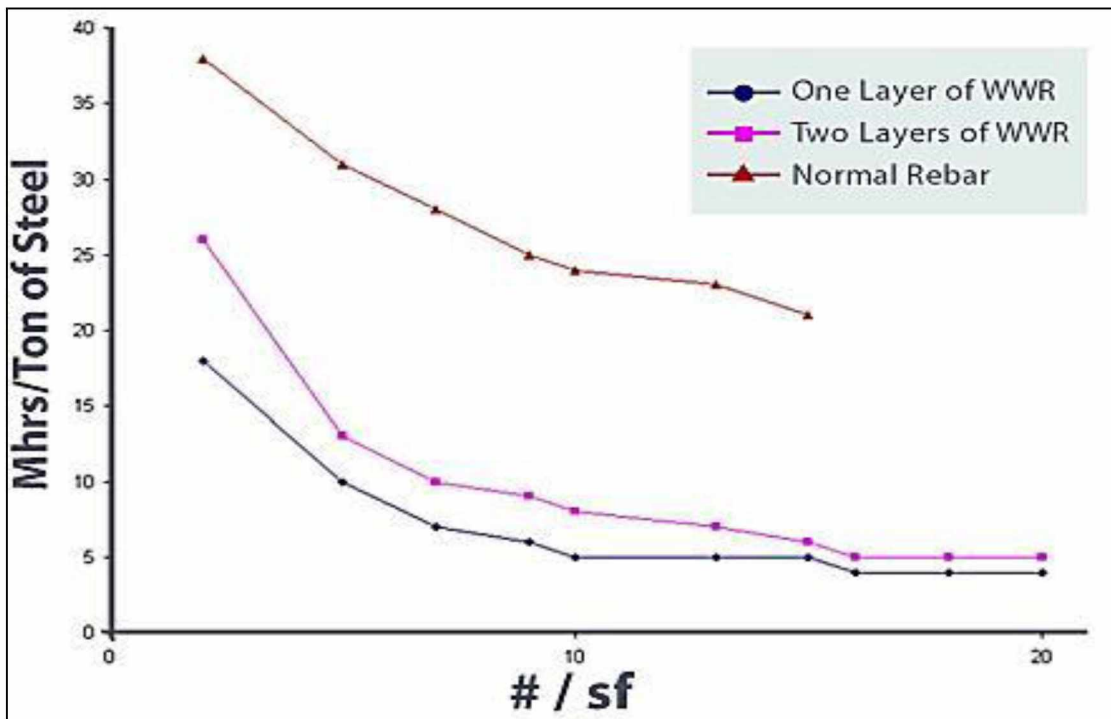


Figure 1.4: Standard Laying Time for Traditional Rebar and Welded Wire Reinforcement
(Arbeitszeitwerte 1977)

Figure 1.5 shows that WWR material cost is usually higher than traditional rebar due to higher fabrication cost, however the installation price is 20% lower than traditional rebar (Bernold and Chang 1992).

Cost Items	Placement Method		
	Traditional Rebar	WWR D12 Manual (8 x 18 ft)	WWR D12 Mechanical (8 x 40 ft)
Material			
Quantity (t)	45.7	44.5	43.0
Unit cost (dollars)	600.00	750.00	750.00
Total base cost (dollars)	27,420.00	33,375.00	32,250.00
Total cost including 10% O&P (dollars)	30,162.00	36,712.00	35,475.00
Labor			
Productivity (man-hours/t)	18.8	4.0	1.4
Crew			
Foreman	1 at \$22.00	1 at \$22.00	1 at \$22.00
Skilled laborers	4 at \$20.00	5 at \$20.00	2 at \$20.00
Unskilled laborers	4 at \$15.00	8 at \$15.00	2 at \$15.00
Crew cost (dollars/hr)	162.00	242.00	92.00
Total crew time (hrs)	96	13	12
Total bare installation (dollars)	15,552.00	3,146.00	1,104.00
Total labor cost including 20% O&P (\$)	18,662.00	3,775.00	1,325.00
Equipment			
Crane (for placement only)	0	0	1
Cost including operator (\$/day)	0.00	0.00	1,182.00
Total equipment cost including 20% O&P (\$)	0.00	0.00	2,128.00
Total work days (work days)	12.0	1.5	1.5
Total cost (\$)	48,824.00	40,487.00	38,928.00
Cost savings (%)		18	21

Figure 1.5: Cost Comparison for Traditional Rebar and Welded Wire Reinforcement (Bernold and Chang 1992)

In the past ten years, some precast/pre-stressed concrete bridges spanning 150 feet (45720 mm) or more have WWR as shear reinforcement along their length. Dr. Maher Tadros at the University of Nebraska developed an I-Girder of 1800 inch (45720 mm), with a depth of 84 inch (2133 mm) and a top flange width of 48 inch (1219 mm). The girder has over two tons of shear reinforcement in its web and flanges. In this girder, typical bridge reinforcing was substituted with WWR (Morcous, Maguire, and Tadros 2011).

1.1.3 Welded Wire Reinforcement Specifications and Nomenclature

A complete unit of WWR mesh is designated as an “item” in the wire industry. An item consists of a group of plain and deformed wires welded together to form a mesh. Size designations of individual wire (plain and deformed) are based on the cross-sectional area of a

given wire. To differ from the traditional rebar industry of using gage numbers to designate wire size, in 1970 the WWR industry decided to use letter-number combinations of wire size. The prefixes “W” and “D” are used in combination with a number. The letter “W” designates a plain wire and the letter “D” denotes a deformed wire. The number following the letter gives the cross-sectional area in hundredths of a square inch. For metric wire, the prefix “M” is added. For example, MW describes metric plain wire and MD metric deformed wire. The wire spacing for metric is given in millimeters (mm), and the cross-sectional areas of the wires are in square millimeters (mm²) (Wire Reinforcement Institute 2006).

For instance, wire designation W10 would indicate a plain wire with a cross-sectional area of 0.10 in² (64.5 mm²). D5 wire would indicate a deformed wire with a cross-sectional area of 0.05 in² (32.3 mm²). The size of wires in welded wire mesh is designated in the same manner. This system has many advantages. With the known cross-sectional area and spacing of the wire, the total cross-sectional area per foot of width can be determined easily. For instance, a W6 wire on 4 inch centers would provide 3 wires per foot with a total cross-sectional area of 0.18 in² per foot of width (116.1 mm² per meter of width). Spacing and sizes of wires are identified by “style” (Wire Reinforcement Institute 2006). For example a typical designation of WWR looks like,

5 X 10 – W12 X W5 in customary U.S. units

127 X 254 – W12 X W5 in metric units

This denotes a unit of WWR in which the spacing and area of longitudinal and transverse wire have been explained in Table 1.1

Table 1.1: Welded Wire Reinforcement Item Description

Description	U.S Customary Units	Metric Units
Spacing of Longitudinal Wire	5 in	127 mm
Spacing of Transverse Wire	10 in	254 mm
Area of Longitudinal Wire	0.12 in ²	77 mm ²
Area of Transverse Wire	0.05 in ²	32 mm ²

WWR may be of deformed or plain or both wires of uniform or non-uniform wire spacing. It is very important to note that the terms longitudinal and transverse are related to the manufacturing process and do not refer to the relative position of wires. Transverse wires are individually welded at right angles as the reinforcement advances through the welder. In some machines, the transverse wire is fed from a continuous coil, in others they are precut to length and hopper fed to the welding position.

There are two types of coatings used on WWR. One is galvanized, which is applied to the cold drawn wire before it is welded into reinforcement. The hot-dipped galvanizing process is similar to that specified in ASTM A641. The other type of coating is epoxy. The epoxy coating is applied after sheets have been welded. The requirements for epoxy coated WWR are provided in ASTM A884. The American Society for Testing and Materials (ASTM) has established specifications for plain and deformed WWR shown in Table 1.2.

Table 1.2: ASTM Specifications (Wire Reinforcement Institute 2006)

Specification	Title
ASTM A82	Cold-Drawn Plain Steel Wire for Concrete Reinforcement
ASTM A185	Welded Plain Steel Wire Reinforcement for Concrete Reinforcement
ASTM A496	Deformed Steel Wire for Concrete Reinforcement
ASTM A497	Welded Deformed Steel Wire Reinforcement for Concrete Reinforcement

As per American Concrete Institute building code (ACI 318), the yield strength values for wires exceeding 60,000 psi (415 MPa) shall be taken by the offset method corresponding to a strain of 0.35 percent. Table 1.3 explains the ASTM requirements for weld shear strength which contribute to the bond and anchorage between wire reinforcement and concrete.

Table 1.3: Weld Shear Strength for WWR (Wire Reinforcement Institute 2006)

Wire Size	Standards	Weld Shear Strength
W 1.2 & over	ASTM A 185	35,000 psi (240 MPa)
W 1.2 & under		-
D 4 to D 45	ASTM A 497	35,000 psi (240 MPa)
D4 & under		-

As per ASTM A370, maximum stretch can be defined as total elongation measuring both elastic and plastic regions. High strength WWR is capable of developing significant strains and exhibits sufficient ductility to redistribute the strains to avoid brittle and shear failure (Purdue 2015).

1.1.4 Welded Wire Reinforcement Manufacturing, Handling and Placing

Chemical composition of WWR is carefully selected for proper welding and desired mechanical characteristics. The high yield strength of WWR is achieved by cold working. WWR is produced on automatic welding machines which are designed for a long, continuous operation. Longitudinal wires are straightened and fed continuously through the machine. Transverse wires, entering from the side or from above the welder, are individually welded at right angles to the longitudinal wires with the required transverse wire spacing.

Longitudinal and transverse wire size, spacing, width, side and end overhang and overall length are controlling variables for manufacturing WWR. The variables listed are dependent on order history, time, and extent to which the machine assembly for special orders needs to be changed. For example, change in longitudinal wire spacing requires repositioning of welding heads which requires a specific time for reassembly.

Bundled WWR for shipping weighs between 2,000 to 5,000 pounds (907 to 2268 kg). Sometimes nesting (flipping alternate sheets) allows for a greater number of sheets to be stacked in a given height and provides additional stability to the bundle. Care should be taken while lifting to prevent from local buckling.

To ensure proper performance of the reinforcement, it is essential that WWR sheets be placed on supports to maintain their required position during concrete placement. The supports (either concrete blocks, steel or plastic “chair” devices, or a combination of these) must be

appropriately spaced in order to work effectively (Wire Reinforcement Institute, 2006). Robotic machines for longitudinal wire feed and welding of wires are shown in Figure 1.6 and Figure 1.7.



Figure 1.6: Longitudinal Wire Fed into Automated Welding Machine (Schnell 2015)

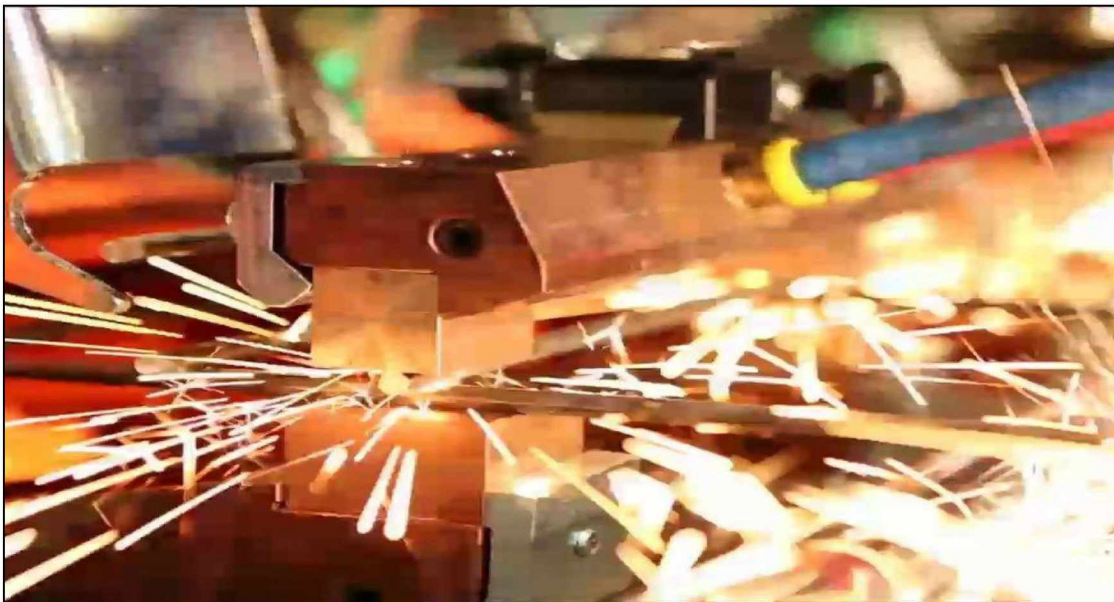


Figure 1.7: Longitudinal and Transverse Wire Welding (Schnell 2015)



Figure 1.8: Crane Handling of Welded Wire Reinforcement Bundle (Schnell 2015)

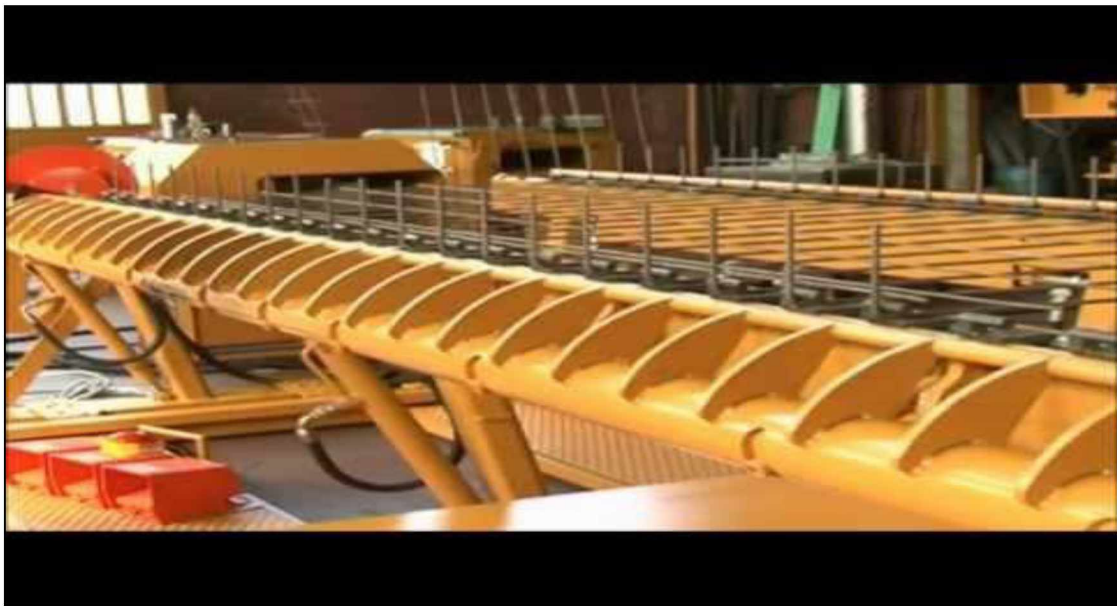


Figure 1.9: Welded Wire Reinforcement Mesh Bending Machine (Schnell 2015)

Crane handling of welded wire mesh with automated mesh bending machines is shown in Figure 1.8 and Figure 1.9.

1.2 Aim and Scope

The aim of the present research was to study the flexural behavior of simply supported welded wire reinforced concrete beams in comparison with concrete beams reinforced with conventional steel bars through numerical analysis. The commercial finite element software ABAQUS was used for this purpose. Also the ability of the software to model non-linear behavior on reinforced concrete beams was investigated.

Initial validation of the non-linear reinforced concrete numerical analysis was carried out based on experimental studies in (Gopinath et al. 2014). In order to evaluate the structural behavior of WWR concrete beams, different aspects such as longitudinal and transverse stirrup configuration were considered and compared with conventional steel reinforced concrete beams. In addition, structurally performing welded wire configuration selected from the concrete beam case is compared with Mexican chair styled reinforcement (Deacero 2015). This part of analysis is performed in a T-beam.

Details on the finite element modeling of a reinforced concrete beam in ABAQUS were presented with concrete damage plasticity model. The results from finite element analysis were compared with calculated results according to ACI 318 design codes.

1.3 Outline of Thesis

In the following chapter, a brief description of research with reference to WWR, used in various structural applications is given. Chapter 3 is an introduction to finite element software ABAQUS and covers exclusively constitutive model and parameters which extract the non-linear behavior of reinforced concrete beams under uniaxial and bi-axial loading conditions.

In chapter 4, geometry, mechanical properties of materials, initial validation combined with mesh convergence are presented with the results. Also, discussions of finite element analysis results of various reinforced concrete beams are followed. Chapter 5 provides conclusions of this study and recommendations for future studies.

Chapter 2 Literature Review

2.1 Impact of Welded Wire Reinforcement in Structural Members

There is a wide range of research pertaining to the use of WWR, as it relates to use on secondary structural components (floor slabs and pavements). There is limited research done on WWR in primary structural components such as beams, columns, and girders. The literature review in this chapter is limited to WWR used in primary structural components. Also, a review on some literatures that pertain to welded wire reinforcements is added.

2.1.1 Welded Wire Reinforcements in Columns

Studies on WWR in columns have convinced contractors and designers to use them in primary structural components. Maximum elongation measurements were 30 to 40 percentage greater than ultimate elongation for WWR, and various test results by Roy H. Reiterman showed that WWR has been tested and proven for its strength, stiffness, ductility, cost effectiveness, and excellent dimension control (Reiterman 1992). Concrete columns confined with WWR have a 40 percentage increase in strength and ductility when they are tested under concentric loading (Razvi and Saatcioglu 1989). As shown in Figure 2.1, considerable gains in strength and ductility were recorded for concrete cores when WWR transverse reinforcement was combined with steel longitudinal bars, after the concrete cover had completely spalled off. Various stirrup configurations and spacing clarified the effectiveness of WWR as transverse reinforcement by increasing shear strength, ductility and toughness of a reinforced concrete member. Volumetric ratio is an important beneficial effect on the stress-strain behavior of concrete, when there is increase in volumetric ratio of WWR, increase in confined strength is observed (Kusuma, Taviu, and Suprobo 2015).

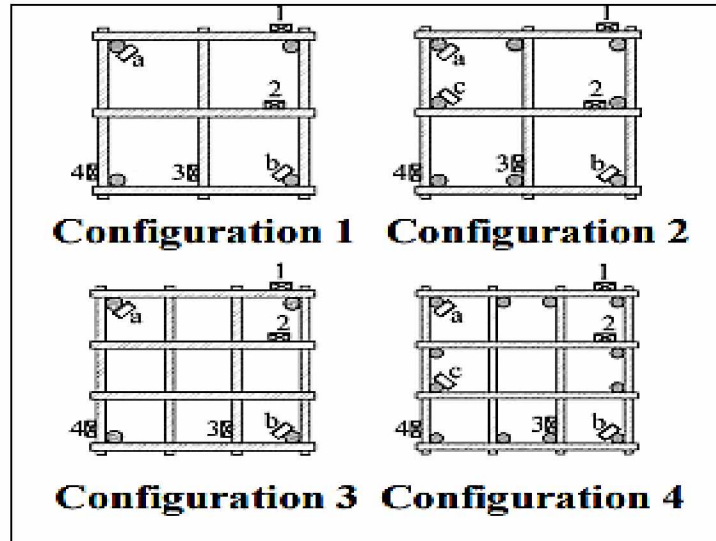


Figure 2.1: Welded Wire Column Reinforcement (Kusuma, Tavio, and Suprobo 2015)

2.1.2 Welded Wire Reinforcements in Beams and Girders

According to Mansur, Lee, and Lee (1988), significant impact on shear strength and diagonal cracking has been observed when tests were conducted on T-beams with bent up WWR coupled with mild steel longitudinal reinforcement with various amounts of shear reinforcement. Figure 2.2 represents a T-beam reinforced with bent-up WWR and mild steel longitudinal reinforcement.

Pre-tensioned, pre-stressed T-beams reinforced with WWR were tested statically to prove effectiveness in shear behavior. The test beams included conventional double legged stirrups, single legged stirrups, and commercially available welded wire fabric. It was found that using deformed welded wire fabric improved the distribution of diagonal cracks (Xuan, Rizkalla, and Maruyama 1987).

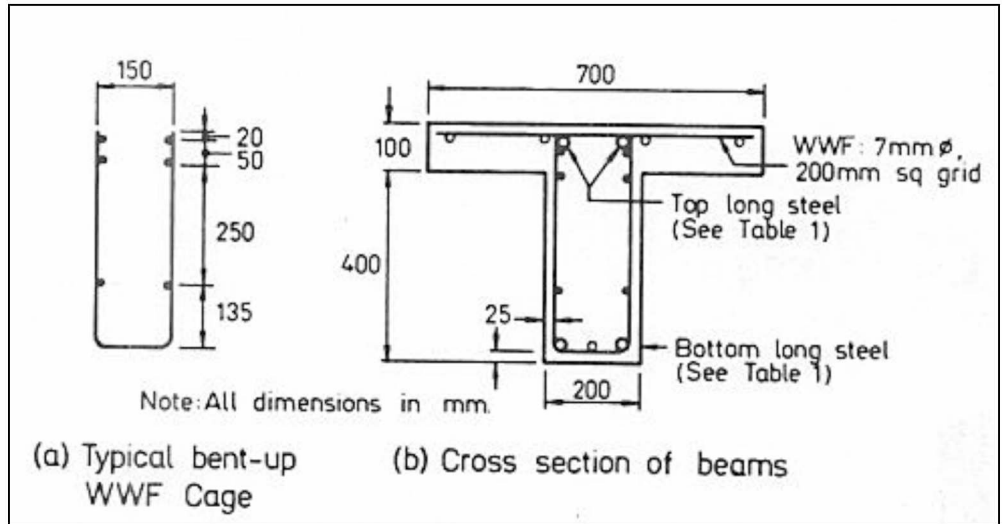


Figure 2.2: Welded Wire Stirrup with Longitudinal Rebar (Mansur, Lee, and Lee 1988)

In a reinforced concrete member having a thin web, the use of welded wire fabric as shear reinforcement is convenient and its performance is as good as stirrups. With the contribution of concrete, the shear strength of a beam was on an average 40 percent greater than the design strength in ACI 318 code and the diagonal tension cracks in the web had an inclination generally less than 30 degrees to the horizontal in general. Whether reinforced with bonded or un-bonded tendons, T-beams with no web reinforcement failed in shear at similar loads (Durrani and Robertson 1987).

2.1.3 Welded Wire Reinforcements in Structural Walls

Reinforced concrete shear walls are widely recognized for providing adequate lateral load resistance, high ductility, drift control and excellent energy dissipation for multistory buildings in seismic regions. The influence of WWR on structural ductility made Paolo Riva and Alberto Franchi test cantilever walls subjected to in-plane cyclic loading. The main objective was to prove whether WWR mesh can provide a sufficient ductility for seismic applications. The test results showed that hot rolled mesh exhibited ductility properties comparable to those reinforced

with mild steel reinforcement. On the contrary, a traditionally cold drawn mesh did not provide enough ductility for seismic applications (Riva, and Franchi 2001).

2.2 Summary

Considerable progress has been made in the past century on coupling WWR with either flexure or shear reinforcement in structural components. In spite of the number of reinforced concrete structures that have been built in combining conventional shear reinforcing with welded wire fabric, there is still no unified solution to predict the structural behavior when both longitudinal and transverse reinforcement are substituted with WWR. This research aims to make full use of WWR in both longitudinal and transverse reinforcement.

Chapter 3 Finite Element Modeling of Reinforced Concrete Beams

3.1 ABAQUS Modeling

This chapter gives a brief description about the nonlinear behavior of concrete and steel followed by different constitutive material models available in ABAQUS as well as the methodology for modeling reinforced concrete beams.

3.2 Non-linear Behavior of Concrete

Concrete may be approximated as an isotropic heterogeneous composite material. It may be considered as homogeneous in a macroscopic sense, as it is made with cement, water and aggregates. Concrete has high compressive strength and low tensile strength, and rather steel is a homogeneous material with well-defined properties (Johnson 1969).

In a reinforced concrete beam, reinforcing bars are embedded in tensile regions of concrete and after concrete cracking. Reinforcing bars resist the internal tensile forces and satisfy the moment equilibrium equation. Structural behavior of a reinforced concrete beam is elastic-plastic. Near failure conditions cause a non-linear response for reinforced concrete beams. This can result in concrete tensile cracking, yielding of reinforcing steel bars and compressive crushing of concrete.

Since the concrete material properties and the properties of reinforcing significantly affect the response, the finite element model must account for the material properties and accommodate the geometric section. Thus, material response during different stages loading affects the overall behavior of the beam.

3.2.1 Uniaxial and Biaxial Behavior

During uniaxial loading, concrete exhibits many micro-cracks due to the variable stiffness of aggregates and mortar. These conditions significantly affect mechanical behavior.

Concrete typically has linear elastic behavior up to 30-40 percent of its compressive strength and beyond that, bond cracks are formed. When stresses are about 70-90 percent of the compressive strength, micro-cracks opens and the cracks continue (Chong 2004).

Depending upon the size and strength of the specimen, the peak stress (f'_{cu}) and strain softening occurs (Kaufmann 1988). As shown in Figure 3.1, the softening part of the stress-strain curve for long specimens are sharper than for short specimens which is due to deformation localization in some regions during unloading of other parts.

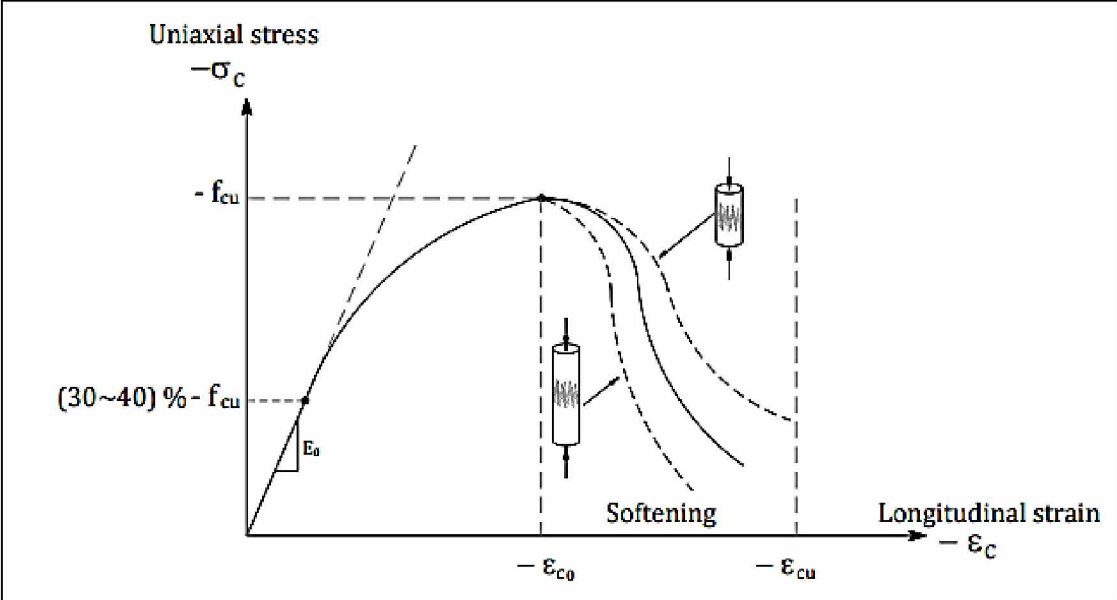


Figure 3.1: Uniaxial Compressive Behavior of Concrete (Kaufmann 1988)

Concrete exhibits a linear response in uniaxial tension up to stresses about 60 – 80 percent of the tensile strength and then behaves softer and highly non-linear (Chong 2004). Beyond the tensile strength, the tensile stress does not suddenly drop to zero due to the brittle nature of concrete. On the contrary, in the weakest regions damage initiates during unloading of

the other parts. Due to interlocking of aggregates, stress can be transferred in the fracture zone across the crack opening direction until a complete crack is formed which cannot transfer any stress, and then complete tensile failure occurs. The concrete during this process undergoes tension softening. The strain in the specimen increases from the effect of the fracture zone and decreases in the rest of specimen that is under elastic unloading. Thus, to evaluate the accurate cracking pattern in concrete, in addition to the strength criterion, energy dissipation in concrete cracking should also be taken into consideration.

Biaxial behavior of concrete is completely different compared to uniaxial behavior. Different studies have been carried out and found that the biaxial strength envelope is enclosed by the proportion of the orthogonally applied stress and the compressive strength, as shown in Figure 3.2. Biaxial stress can be achieved through three different loading forms: biaxial tension, biaxial compression and tension-compression (Kupfer and Gerstle 1973).

Under biaxial compression, the stress strain curve is the same as under uniaxial tension, but compressive strength is up to 25 percent greater due to lateral compressive stress.

The maximum biaxial compressive strength (σ_{2c}) can be calculated from Equation 3.1 suggested by Kupfer and Gerstle,

$$\sigma_{2c} = \frac{1 + 3.65\alpha}{(1 + \alpha)^2} f'_c \quad (3.1)$$

where, f'_c is the compressive strength of concrete and α is a factor calculated according to Equation 3.2,

$$\alpha = \frac{\sigma_1}{\sigma_2} \quad (3.2)$$

where, σ_1 and σ_2 are the principal major and minor stresses.

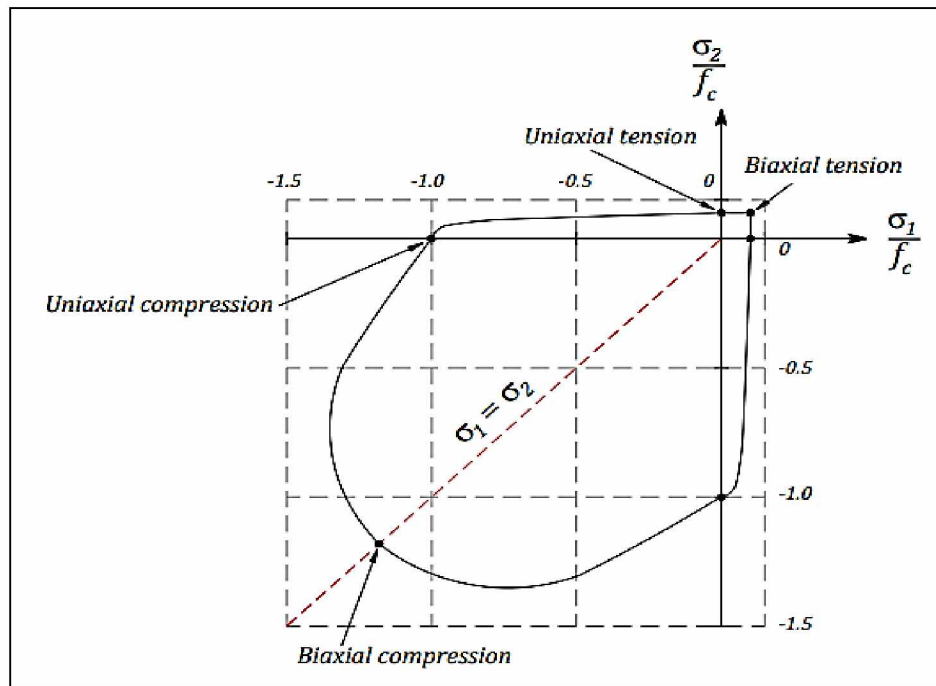


Figure 3.2: Yield Surface in Plane Stress (Kupfer and Gerstle 1973)

3.3 Non-linear Modeling of Reinforced Concrete Beam

To accurately evaluate the structural behavior of reinforced concrete structures, the FE method should be coupled with precise representation of constitutive models. There are three material models for analyzing concrete in ABAQUS. They are concrete smeared cracking model, concrete damaged plasticity model, and brittle cracking model (Hibbitt, Karlsson, and Sorensen 2013).

The concrete smeared cracking model is suitable for cases that describe tensile cracking or compressive crushing. In fact, cracking is the most important aspect of this model. The concrete damage plasticity model considers the stiffness degradation of material as well as

stiffness recovery effects under monotonic and cyclic loading. The brittle cracking model is applicable for cases where tensile cracking should be considered. In other words, this model considers anisotropy due to cracking of the material. In this study the focus is on concrete damage plasticity models which are based on non-linear fracture mechanics theory (Hibbitt, Karlsson, and Sorensen 2013).

Early plasticity theory was developed for expressing the behavior of ductile materials such as metal. Later it got considerably modified to also represent the non-linear behavior of reinforced concrete by defining dense micro-cracks in the material.

A standard plasticity model is based on three conditions: a yield surface, a hardening rule, and a flow rule. When stresses in a material reach the yield surface, plastic deformation starts and then the hardening rule governs the loading surface evolution. During this step, a flow rule with a plastic function controls the strain evolution rate. According to the plasticity theory, total strain rate consists of elastic and plastic components as shown in Equation 3.3.

$$\dot{\epsilon} = \dot{\epsilon}_e + \dot{\epsilon}_p \quad (3.3)$$

where $\dot{\epsilon}_e$ and $\dot{\epsilon}_p$ are the elastic and plastic strain rates, respectively. Equation 3.4 presents a relationship between the stress rate and elastic strain rate, and D_e is a symmetrical linear elastic constitutive matrix.

$$\dot{\sigma} = D_e (\dot{\epsilon} - \dot{\epsilon}_p) \quad (3.4)$$

Equation 3.5, defines the hardening or softening modulus, h

$$h = - \frac{1}{\lambda} \frac{\partial f}{\partial K} k$$

(3.5)

where k , is an isotropic hardening or softening plasticity function and $\dot{\lambda}$ is a scalar value which indicates the magnitude plastic flow.

The earliest study on damage plasticity model was performed by A. Chen and W. Chen. According to them the concrete behaves linear elastic at high stress levels (Chen and Chen 1975) which was criticized by many professionals. Later Han and Chen developed a non-uniform hardening plasticity model, based on associated flow rule, which assumed an unchanged failure surface during the loading process (Han and Chen 1985). In addition to the work done by Han and Chen, an energy based composite plasticity model was introduced by Feenstra and De Borst (1966). This model was designed for plain and reinforced concrete structures subjected to monotonic loading conditions according to two criteria, a Rankine yield criterion and a Drucker-Prager yield criterion (Feenstra and De Borst 1996). Then, the energy model based on the crack band theory was incorporated with the plasticity model and a model was developed for concrete structures subjected to tension-compression biaxial stresses (Chong 2004).

3.4 Material Model Properties

Concrete damage plasticity model has a capability to represent the inelastic behavior of concrete by adopting isotropic damage elasticity with isotropic tensile and compressive plasticity behavior.

3.4.1 Concrete Damage Plasticity Parameters

In ABAQUS, concrete damaged plasticity model requires various parameters. The dilation angle, ψ is measured in p-q plane and should be defined to calculate the inclination of the plastic flow potential in high confining pressures. The dilation angle is equal to the friction angle in low stresses. In higher levels of confinement stress and plastic strain, dilation angle is

decreased. Maximum value of $\psi_{\max}=56.3^\circ$ and minimum value of ψ_{\min} is close to 0° . Upper values represent a more ductile behavior and lower values show a more brittle behavior (Hibbitt, Karlsson and Sorensen 2013).

The flow potential eccentricity, ε , is a small positive number, which defines the range that the plastic potential function closes to the asymptote as shown in Figure 3.3. The default value in ABAQUS is 0.1 and indicates that the dilation angle is almost constant in a wide range of confining pressure. In a higher value of ε , with reduction of confining pressure, the dilation angle increases more rapidly. Very small values can cause convergence problems (Hibbitt, Karlsson and Sorensen 2013).

The proportion of initial equibiaxial compressive yield stress and initial uniaxial compressive yield stress is defined as f_{b0}/f_{c0} . The default value in ABAQUS is 1.16.

The ratio of the second stress invariant in the tensile meridian to compressive meridian for any defined value of the pressure invariant at initial yield is K_c . This parameter is used to define the multi-axial behavior of concrete and the default value in ABAQUS is 0.667.

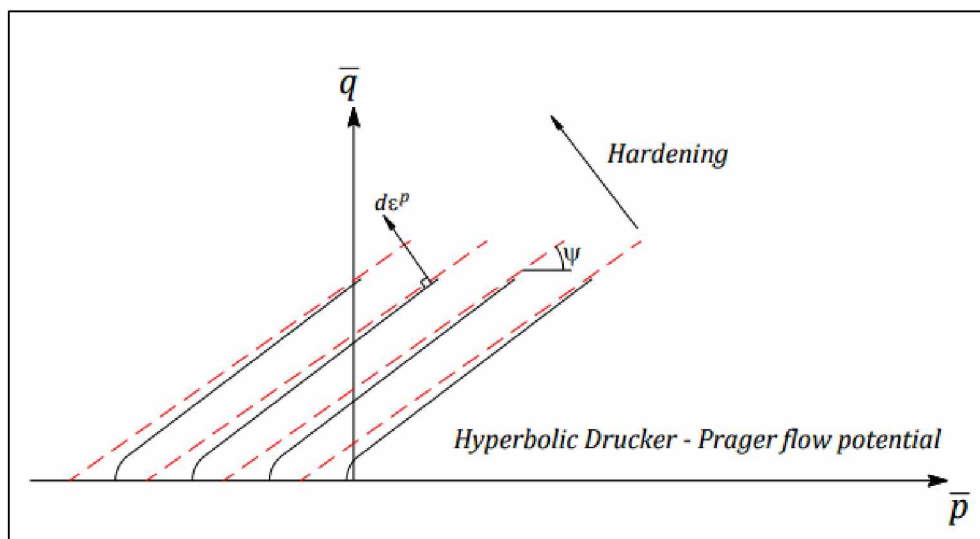


Figure 3.3: Hyperbolic Plastic Flow Rule (Hibbitt, Karlsson and Sorensen 2013)

The viscosity parameter, μ , does not affect the ABAQUS/Explicit analysis but contributes to convergence in an ABAQUS/Standard analysis. To take the degradation of concrete into consideration after cracking, damage parameters should also be defined. The compressive damage parameter, d_c , has a critical effect on the convergence rate in excessive damage. It has to be defined in the range of $0 < d_c \leq 0.99$. The tension damage parameter, d_t , is in the range of $0 < d_t \leq 0.99$. The recommended maximum value is 0.9 as for the compression damage parameter. (Hibbitt, Karlsson and Sorensen 2013).

Concrete beams have been modeled as a C3D8 element, an eight noded three dimension continuum element. The material properties of concrete used in the present study, included a compressive strength of 4500 psi (30 MPa or M30), a modulus of elasticity of 4066840 psi (28,000 MPa) and a Poison's ratio of 0.2.

Parameters for concrete damage plasticity model were adopted from experimental results in Jankowaik and Lodygowski (2006), which also includes the concrete compressive stress and strain values shown in Table 3.1 and Table 3.2

Table 3.1: Concrete Damage Plasticity Parameters (Jankowaik and Lodygowski 2006)

Concrete Damage Plasticity Parameters	Value
Dilation angle, ψ	31°
Flow potential eccentricity, ε	0.1
Initial biaxial/uniaxial ratio, f_{b0}/f_{c0}	1.16
Ratio of second stress invariant, K_c	0.667
Viscosity Parameter, μ	0

Table 3.2: Concrete Compressive Stress versus Strain (Jankowaik and Lodygowski 2006)

Compressive Stress (MPa)	Strain
15.0000	0
20.1978	0.0000747
30.0061	0.0000988
40.3038	0.0001541
50.0076	0.0007615
40.2361	0.0025575
20.2361	0.0056754

3.4.2 Reinforcement Properties

Reinforcement can be modeled with different methods including smeared reinforcement in the concrete, cohesive element method, discrete truss, or beam elements with the embedded region constraint or built-in rebar layers (Hibbitt, Karlsson and Sorensen 2013).

Rebar defines the uniaxial reinforcement levels in membrane, shell, and surface elements. One or multiple layers of reinforcements can be defined. For each layer, the rebar layer name, the cross sectional area of each reinforcement layer, and the rebar spacing in the plane of definition should be defined (Hibbitt, Karlsson and Sorensen 2013).

In the present study, reinforcement is modeled as three dimensional beam elements. A beam element is a common way of reinforcement modeling for which the only required input is the shape and diameter of the rebar, and also takes into account dowel effect. According to

Hibbitt, Karlsson, and Sorensen, the effect of bond slip is also considered in the embedded region modeling method but this effect is considered by tension stiffening behavior of concrete.

Since steel is a much more homogeneous material, relative to concrete, a typical stress/strain curve was used to define steel plasticity and is presented below. Figure 3.4 shows a stress-strain graph of both mild steel bars and WWR. Stress strain parameters of traditional steel (Grade 60 or 415 MPa) have been adopted from experiments done by Jankowaik and Lodygowski (2006). Stress strain parameters for welded wires (Grade 80 or 550 MPa) have been obtained from Wire Reinforcement Institute (Wire Reinforcement Institute 2006).

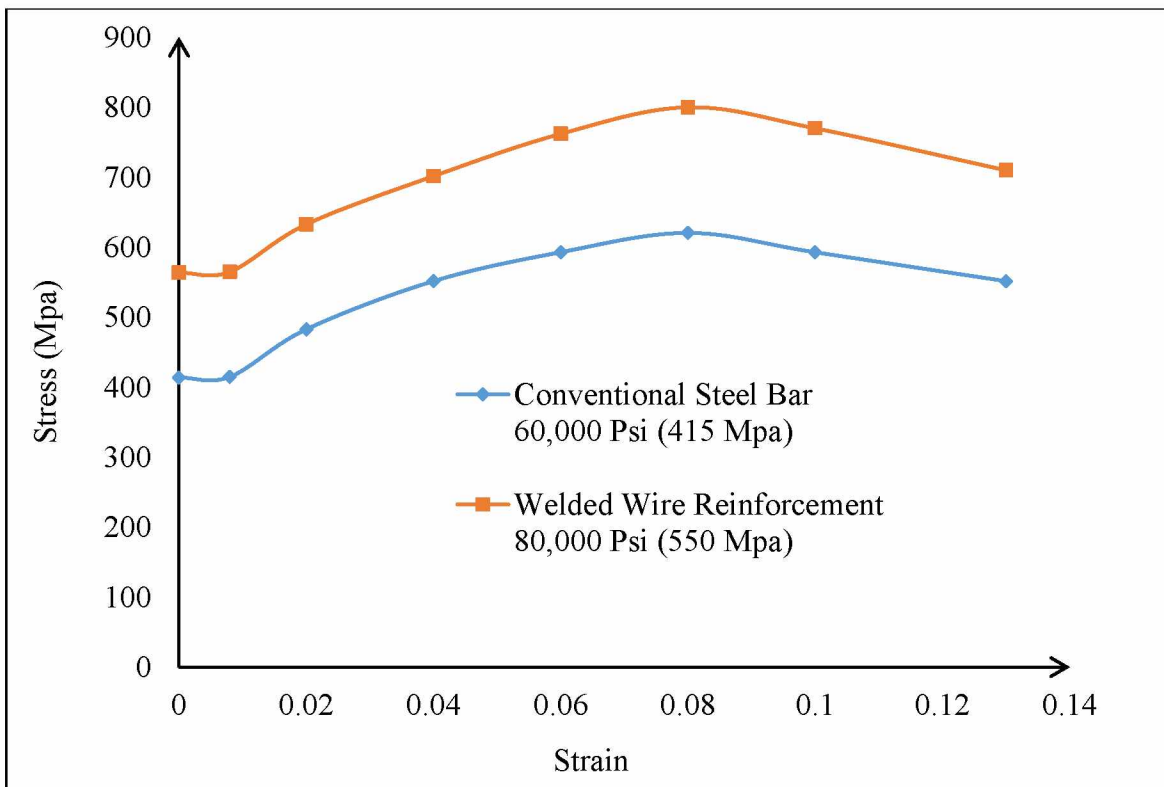


Figure 3.4: Conventional (60 Ksi) and WWR (80 Ksi) Steel Stress Strain Graph

3.5 Convergence Analysis

Different convergence problems may occur during modeling and analyzing reinforced concrete structures. In addition, there are several methods to solve the problems considering the definition of mesh, boundary condition, and loads. Some common solutions for convergence problems are mentioned in this part of the document.

Time step increment: In time step definition in ABAQUS, the minimum time increment should be defined lower than the default values and thus, the maximum number of increments should be increased. Apart from solving the convergence problems, it also leads to more accurate results. However, it needs high computational capacity and is time consuming.

Mesh convergence: In places where reinforcement and concrete nodes coincide, convergence problems occur due to distortion of elements with less stiff material because of high reinforcement stress. Thus, coinciding reinforcement and concrete element nodes should be avoided.

Material instability: The input values for concrete and steel might have a huge impact in convergence of the model. The analysis will be aborted if the input properties are unstable. In a concrete damage plasticity model, the viscosity parameter can affect the convergence problem. For static problems, convergence difficulties still exist. It is recommended to use the concrete damage plasticity model in ABAQUS/Explicit (Hibbitt, Karlsson and Sorensen 2013).

“This page intentionally left blank”

Chapter 4 Numerical Analysis of Concrete Beams Reinforced with Traditional and Welded Wire Reinforcement

4.1 Introduction

This chapter includes numerical analysis of concrete beams reinforced with traditional mild steel reinforcement and WWR. Different parametric analysis of this study includes geometry of reinforcement configuration, mechanical properties of materials, and different loading conditions. Modeling details have been explained briefly.

Also, since it is a numerical study, it is essential that modeling accuracy is ensured. Therefore, an initial validation analysis was done to ensure its accuracy. A simply supported reinforced concrete beam spanning 60 inch (1500 mm) with cross sectional dimensions 4 X 12 inch (100 X 150 mm) was subjected to a four point bending test and its flexural performance was observed (Gopinath et al. 2014). To capture numerical accuracy, the reinforced concrete beam used in the experiment was virtually simulated in ABAQUS, and its flexural performance was observed. Later, the results from both investigations were compared accompanied with a mesh convergence study to verify the accuracy of the finite element model.

The reinforced concrete beam of configuration 1 (B1RC) has been designed as an under reinforced beam to fit the four point bending experimental set up at the University of Alaska Fairbanks. Single reinforced concrete beam (B1RC) of grade 60 (60,000 psi) has been converted to grade 80 (80,000 psi) welded wire reinforced concrete beams (B2WWR, B3WWR, and B4WWR). By the usage of automatic bending machine, stirrups were modeled to be bent in a fashion shown in Figure 4.3 and Figure 4.4. The flexural reinforcing was distributed equally in both tension and compressive faces of the beam. In order to provide perfect bonding and load transfer between concrete and steel, an extra leg of stirrup has been extended in the form

configuration 3 (B3WWR). WWR concrete beam of configuration 4 (B4WWR) has been modeled as a rectangular stirrup with all the flexural reinforcing lying on the tension side of the beam. Being wire reinforced beam, the reinforcing wire has been chosen to be small to accommodate a perfect load transfer mechanism between concrete and steel.

First, different types of stirrup configuration grids B2WWR, B3WWR, and B4WWR (Welded Wire Reinforced Concrete Beam Configuration 2, 3, and 4 shown in Figure 4.3, Figure 4.5) are compared with a traditionally reinforced beam B1RC (Reinforced Concrete Beam Configuration 1 shown in Figure 4.2). Second, structurally performing welded wire configuration selected from the previous case is compared with a Mexican chair styled reinforcement (Deacero 2015). This part of the analysis is done in a T-beam. Mechanical properties of concrete and steel are common for both cases subjected to four point and uniformly distributed load cases.

The parametric study includes variables such as various stirrup configuration grids, ductility ratio, failure modes compared between rectangular beams reinforced with traditional rebar, and welded wire reinforcement when subjected to four point and uniformly distributed loading conditions.

Simply supported rectangular concrete beam B1RC, B2WWR, B3WWR, B4WWR (Figure 4.3, Figure 4.5) with a total length of 192 inch (4877 mm) have a rectangular cross section with 8 inch (203 mm) width and 12 inch (305 mm) height.

The beam is subjected to two concentrated loads, spaced 60 inch (1524 mm) giving a shear span of 5 feet (1524 mm) as shown in Figure 4.1.

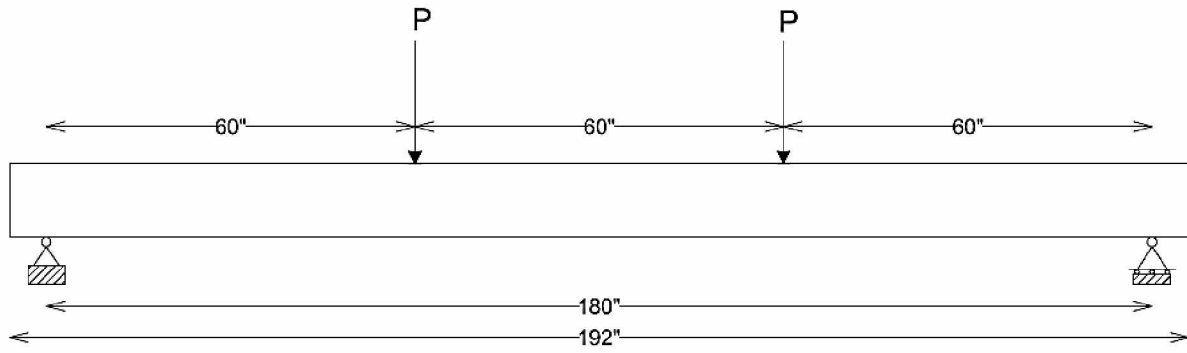


Figure 4.1: Four Point Bending Test Setup

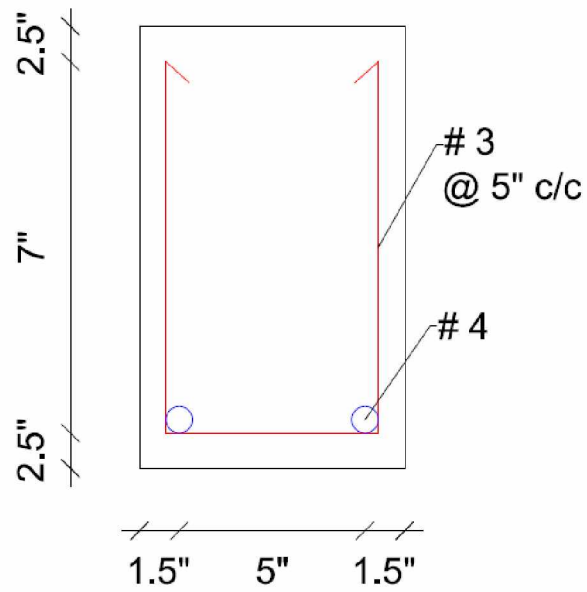


Figure 4.2: Cross Sectional Details of Beam B1RC

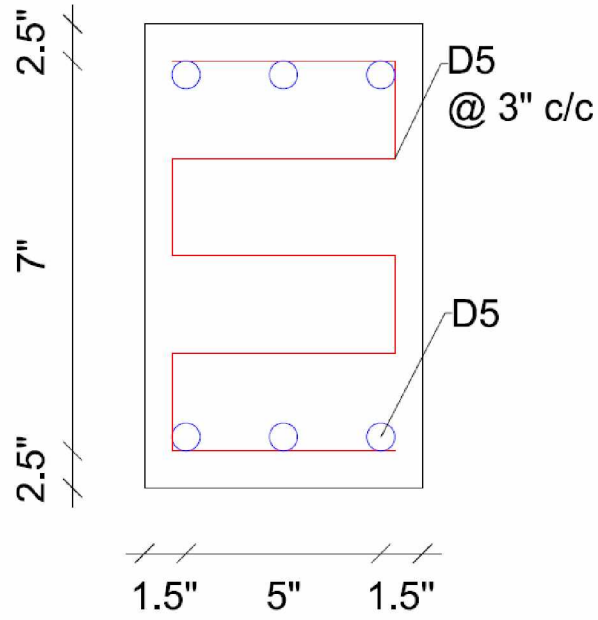


Figure 4.3: Cross Sectional Details of Beam B2WWR

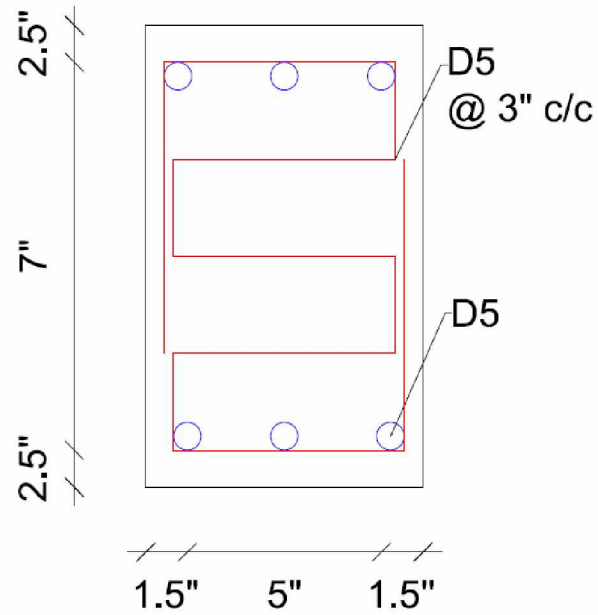


Figure 4.4: Cross Sectional Details of Beam B3WWR

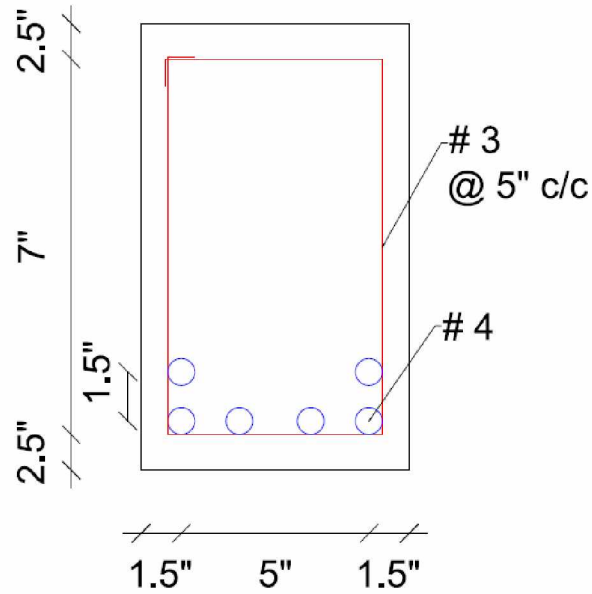


Figure 4.5: Cross Sectional Details of Beam B4WWR

Table 4.1: B1RC, B2WWR, B3WWR, B4WWR Beam Properties

Beam Designation / Specifications	B1RC	B2WWR	B3WWR	B4WWR
Length (in)	192	192	192	192
Width (in)	8	8	8	8
Depth (in)	12	12	12	12
Concrete Grade (psi)	4500	4500	4500	4500
Steel Grade (psi)	60,000	80,000	80,000	80,000
Area of steel (in ²)	0.4	0.3	0.3	0.3
Longitudinal Reinforcement	#4	D5	D5	D5
No.of. Longitudinal Reinforcement	2	6	6	6
Shear Reinforcement	#3	D5	D5	D5
Spacing of Shear Reinforcement (in)	5	3	3	3
Concrete Cover Top and Bottom (in)	2.5	2.5	2.5	2.5
Concrete Cover Left and Right (in)	1.5	1.5	1.5	1.5

Simply supported T-beams, TB1MS (T-beam with Mexican style reinforcing configuration shown in Figure 4.7) and TB2WWR (T-beam with WWR configuration shown in Figure 4.8) have a flange width of 24 inch (610 mm), slab thickness of 2 inch (51 mm), web width of 8 inch (203 mm) and web height of 10 inch (254 mm) spanning 192 inch (4877 mm). Table 4.2 explains TB1MS and TB2WWR beam properties in detail.

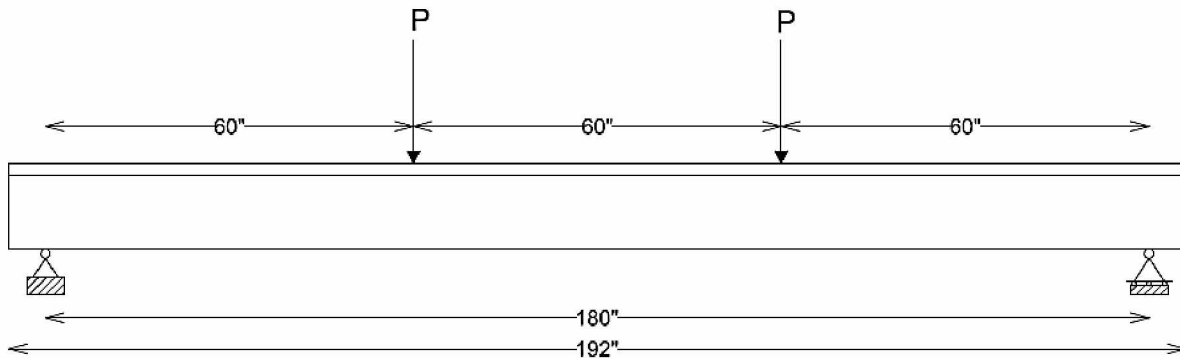


Figure 4.6: Four Point Bending Test Setup of T - Beam

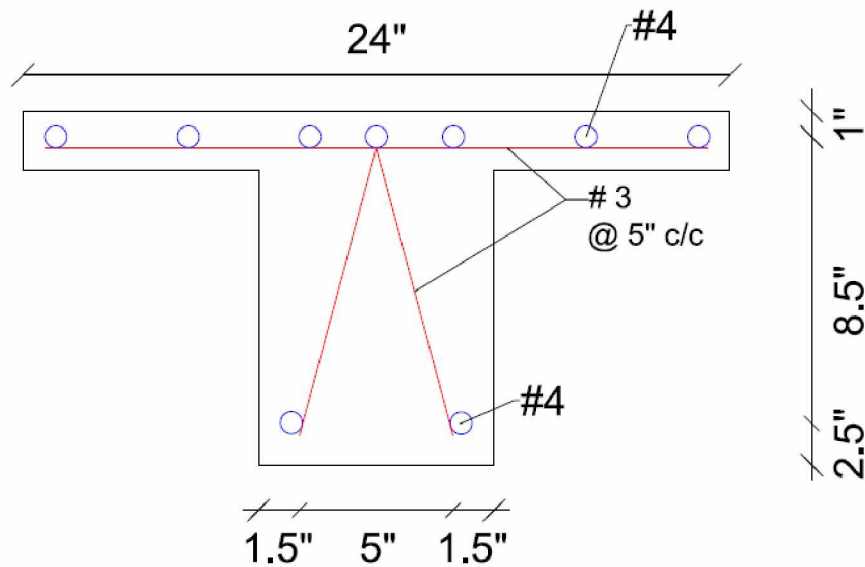


Figure 4.7: Cross Sectional Details of T- Beam TB1MS

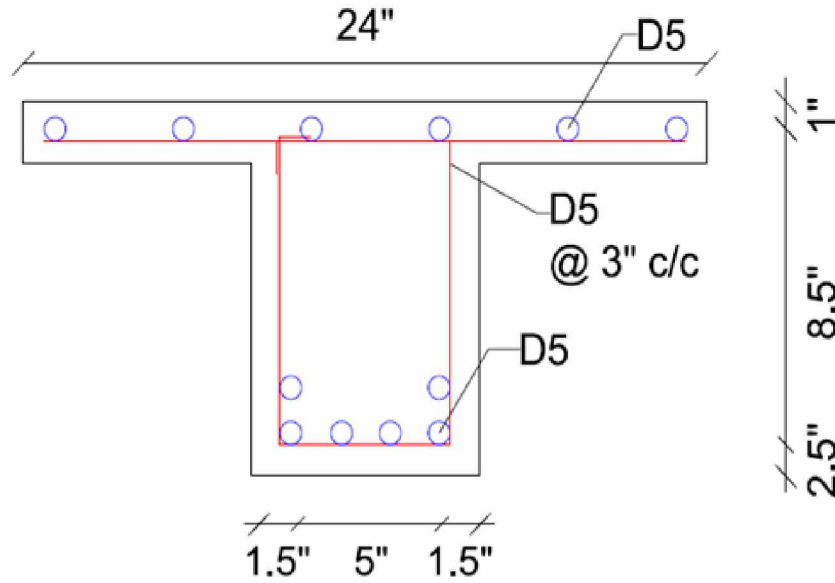


Figure 4.8: Cross Sectional Details of T- Beam TB2WWR

Table 4.2: TB1MS and TB2WWR Beam Properties

Beam Designation / Specifications	TB1MS	TB2WWR
Length (in)	192	192
Flange Width (in)	24	24
Web Width (in)	8	8
Depth (in)	10	10
Slab Thickness (in)	2	2
Concrete Grade (psi)	4500	4500
Steel Grade (psi)	60,000	80,000
Area of steel (in ²)	0.4	0.3
Longitudinal Reinforcement	#4	D5
No.of. Longitudinal Reinforcement	2	6
Shear Reinforcement	#3	D5
Spacing of Shear Reinforcement (in)	5	3

4.2 Initial Validation and Mesh Convergence

Experiments have been done on a simply supported reinforced concrete beam spanning 60 inch (1500 mm) with cross sectional dimensions 4 X 12 inch (100 X 150 mm), under four point bending test in order to observe its flexural performance (Gopinath et al. 2014). Figure 4.9, Figure 4.10, and Figure 4.11 show the cross sectional details and four point bending test setup for the experimental beam. The load versus deflection graph for the experimental beam is presented in Figure 4.15, which then is used to compare the accuracy of the modeling results.

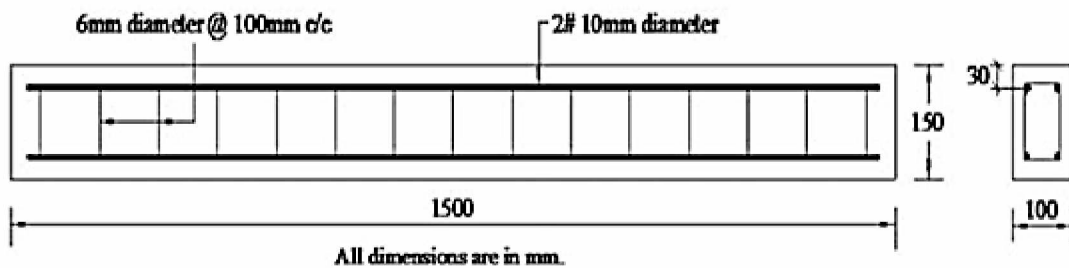


Figure 4.9: Experimental Beam Cross Section (Gopinath et al. 2014)

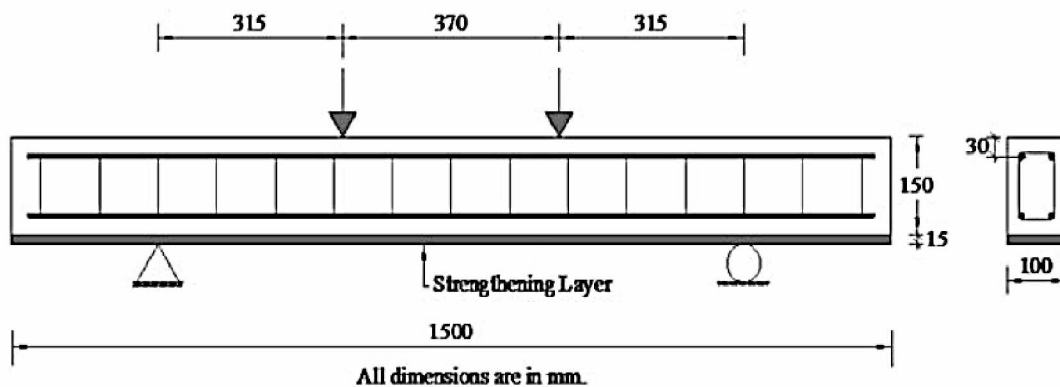


Figure 4.10: Four Point Bending Test Setup for Experimental Beam (Gopinath et al. 2014)



Figure 4.11: Beam when Placed in the Test Setup (Gopinath et al. 2014)

The beam used in the test has been virtually simulated in ABAQUS for a four point bending test. As discussed earlier, the concrete beam has been modeled with eight noded, three dimension continuum elements, while the reinforcing bars have been modeled with three dimension beam elements. Concrete damage plasticity model and elastic plastic model were adopted for concrete and steel, respectively to implement the nonlinear behavior. The assembly of longitudinal and transverse reinforcement has been done, and to ensure proper bonding between concrete and steel, embedded interaction module has been chosen to virtually simulate reinforced concrete beam behavior.

The finite element modeling has a step size which literally controls iterations during the analysis. The minimum step size was used and as a result, the analysis converges by iterative process. For a perfectly elastic plastic material, if the load applied is more than the yield strength,

the model diverges. So, the beam has been subjected to a deflection under the loading point with a deflection rate of 1.182 inch / sec (30 mm/sec). The same rate of deflection had been adopted in the experimental beam as well. Since it is a simply supported beam, hinge and roller support boundary conditions were specified on both ends of the beam. Vertical and horizontal reaction is constrained for the hinge support and only vertical reaction is constrained for roller support boundary condition.

The numerical solution will tend to converge towards a unique value by refining the mesh density. It is important to use a sufficiently refined finite element mesh so that the results from ABAQUS analysis are adequate. Sometimes coarse mesh yields a value which is far from the actual expected outcomes. Fine mesh tends to produce a satisfactory result but it requires quite a lot of resources and time to run the model. A model is said to be convergent where further mesh refinement does not affect the accuracy of solution. Mesh refinement comes by experience and it is always advisable to perform a mesh convergence test before starting an analysis. Different mesh sizes 1 inch (25 mm), 2 inch (50 mm), and 3 inch (75 mm) were incorporated to determine the optimized mesh size. Validation analysis and mesh convergence has been done parallel with the experimental beam to optimize the finite element model.

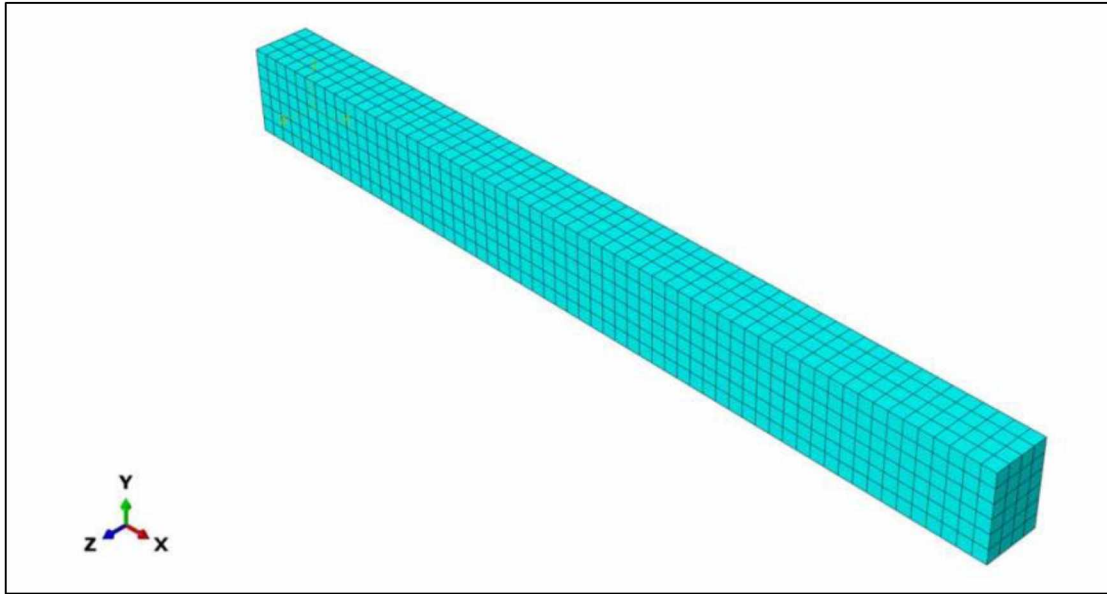


Figure 4.12: Experimental Beam Mesh Size 1 inch (25 mm)

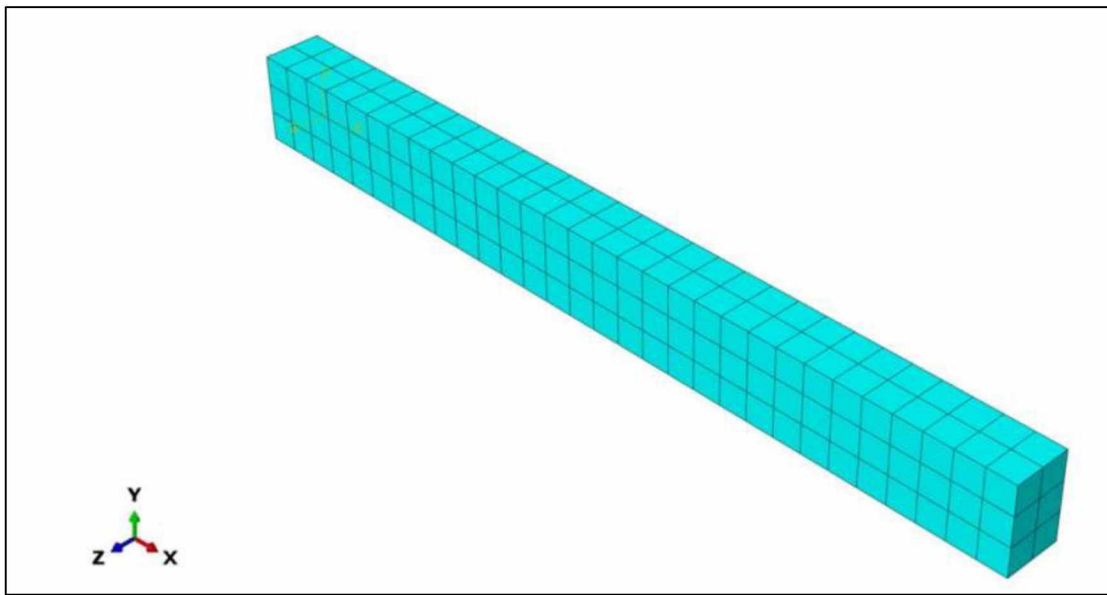


Figure 4.13: Experimental Beam Mesh Size 2 inch (50 mm)

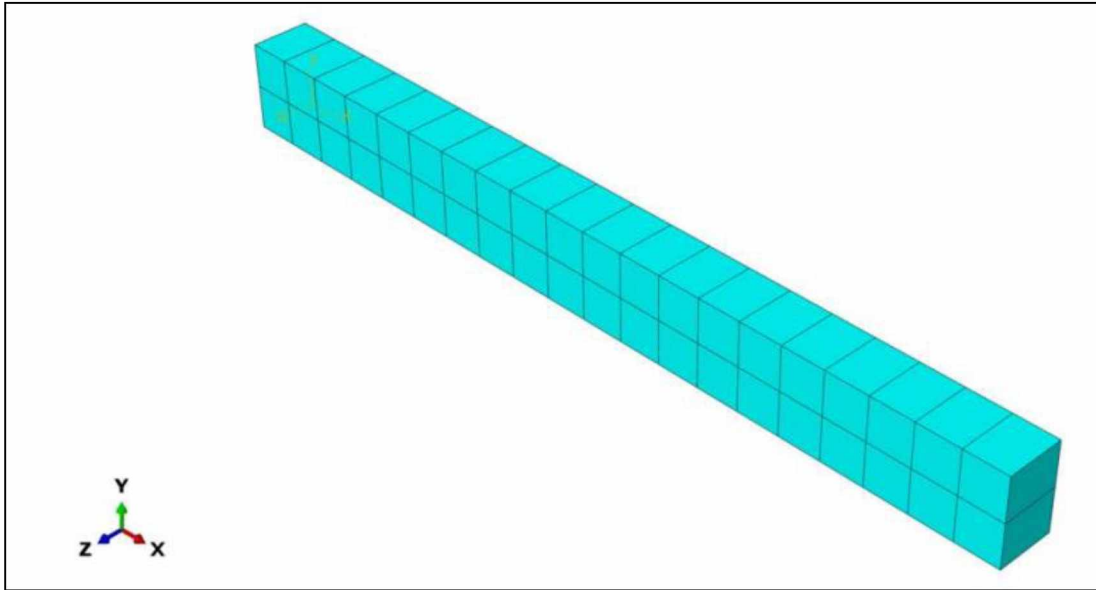


Figure 4.14: Experimental Beam Mesh Size 3 inch (75 mm)

This is done by using the three different mesh densities shown in Figure 4.12, Figure 4.13, Figure 4.14. The cross sectional details of the beam are shown in Figure 4.9, and the mesh element types with number of nodes for different mesh density are tabulated in Table 4.3.

Table 4.3: Various Mesh size and Element Type for Experimental Beam

Mesh Size (in)	Total no. of Nodes	Total no. of Beam Elements	Beam Element Type	Total no. of Rebar elements	Rebar Element Type
1	2543	1440	Hexahedral	404	Line
2	578	180		202	
3	266	40		136	

Since the available experimental data and modeling parameters are in SI units, the finite element analysis was carried out in SI units and the results are presented in SI units for the initial validation study. Analysis results apart from validation study have been presented in U.S Customary units for better understanding.

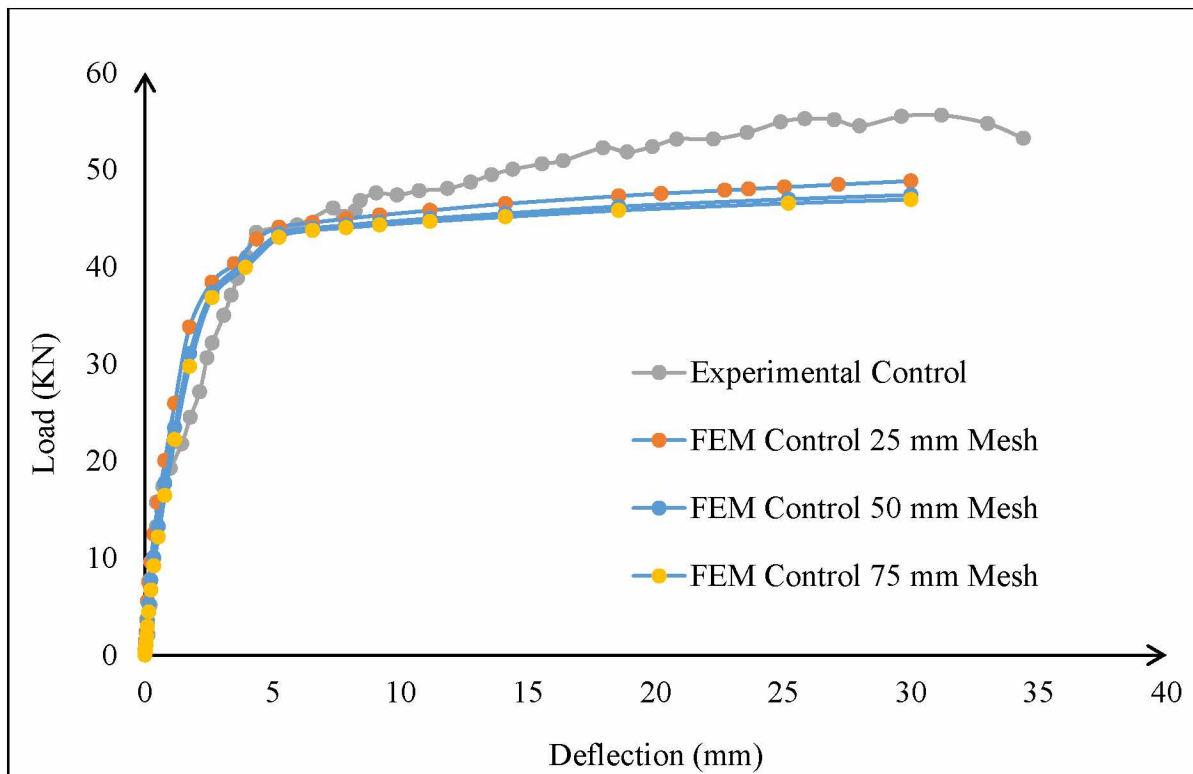


Figure 4.15: Load versus Deflection Graph for Experimental Beam

From Figure 4.15, the result of modeling is in good agreement with the experimental result. Both experimental and analysis results follow the similar load carrying curve. The failure mode of this beam was yielding of steel bars which is due to the under reinforced condition of the beam. It is shown that both analysis results and experimental result graphs have rather the same slopes until yielding of steel bars and the same path until failure. Based on the

comparisons, it can be concluded that the modeling procedure and definition of material in modeling of the concrete beam have the required accuracy and precision to present the non-linear behavior of the concrete material.

For the 3D analysis of reinforced concrete beam with different mesh density, the available resource often dictates a practical limit on mesh density to use. Coarse mesh is often adequate to predict trends and to compare how different concepts behave. Fine mesh is used in areas of high stress gradients. But it is always advisable to use a uniform mesh all over the model. By comparing the results under the mesh convergence study (Table 4.3 and Figure 4.15), 2 inch (50 mm) finite element mesh size has 578 nodes and the run time is minimum when compared to other mesh densities. So a mesh size of 2 inch (50 mm) has been chosen for the forthcoming analysis. Also for a better understanding and accuracy in mesh convergence study, control beam B1RC is subjected to four point bending test under various mesh densities. The various mesh densities are presented in Figure 4.16, Figure 4.17, and Figure 4.18.

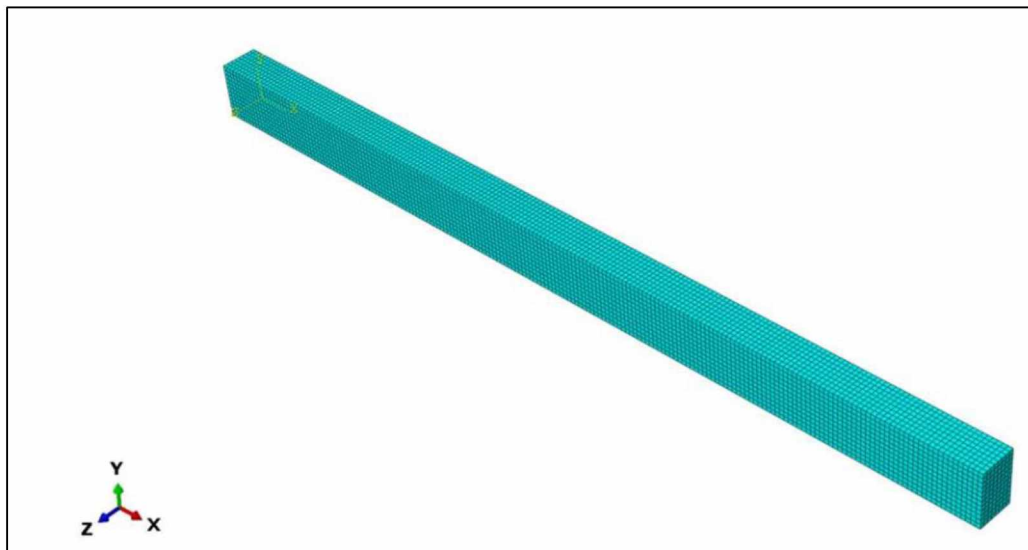


Figure 4.16: Reinforced Concrete Beam (B1RC) of 1 inch (25 mm) Mesh Size

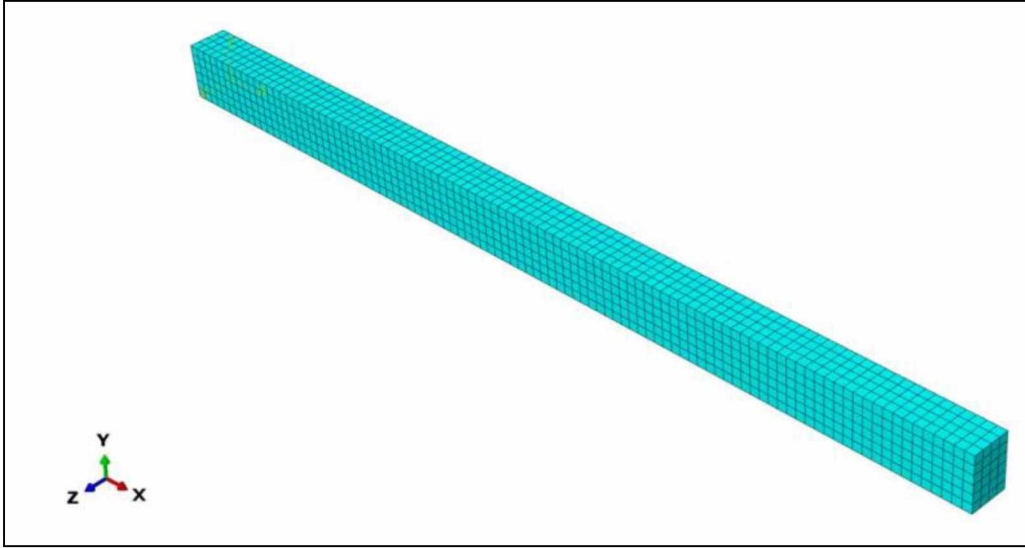


Figure 4.17: Reinforced Concrete Beam (B1RC) of 2 inch (50 mm) Mesh Size

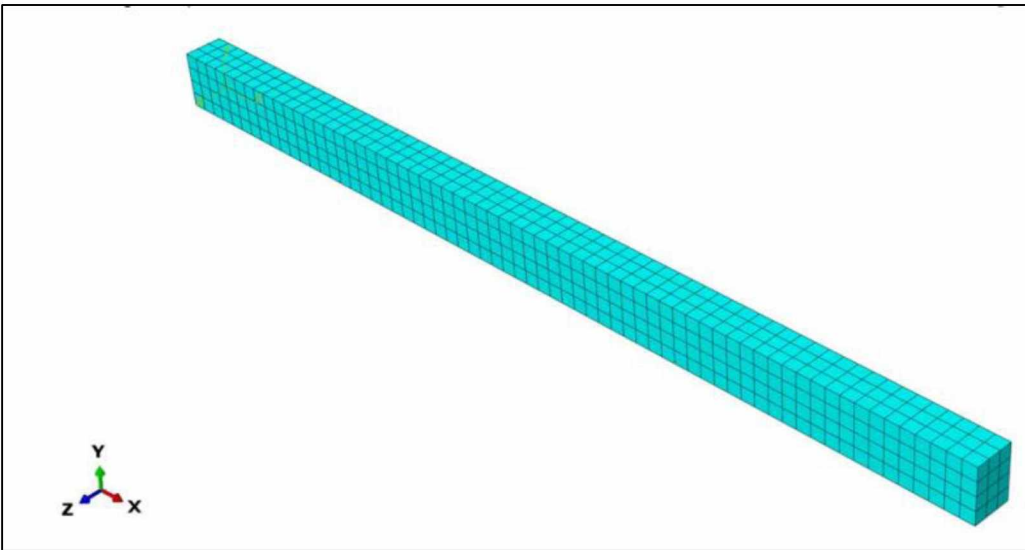


Figure 4.18: Reinforced Concrete Beam (B1RC) of 3 inch (75 mm) Mesh Size

Table 4.4: Various Mesh size and Element Type for Beam B1RC

Mesh Size (in)	Total no. of Nodes	Total no. of Beam Elements	Beam Element Type	Total no. of Rebar elements	Rebar Element Type
1	24020	18720	Hexahedral	1050	Line
2	4081	2352		578	
3	1696	780		338	

The results include load versus mid-span deflection graphs for different mesh density and to make sure that the selected 2 inch (50 mm) mesh size works for all the beams. Load versus mid-span deflection values have been extracted from the nodes that face on the compressive side of the reinforced concrete beam. From Table 4.4, 2 inch (50 mm) mesh size tends to have a mid-range of nodes which is not over or under predicted. Figure 4.19 also represents that by using 2 inch (50 mm) mesh size. There is no unified change in the load under specified deflection. So to be consistent 2 inch (50 mm) mesh size has been made use in all forthcoming analysis.

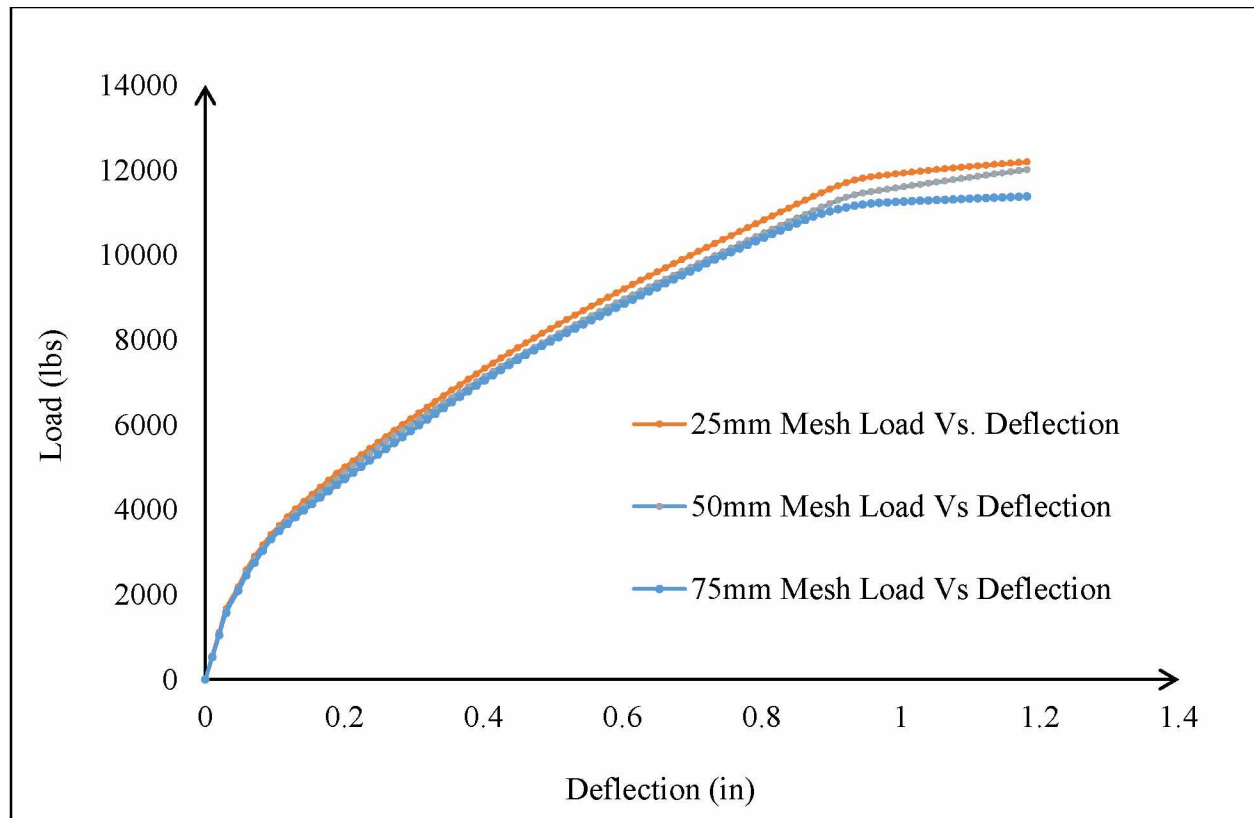


Figure 4.19: Load versus Deflection Graph for Beam B1RC

4.3 Analysis of Welded Wire Reinforcement Grids in Reinforced Concrete Beams

For the case of different types of stirrup configuration grids, B2WWR, B3WWR, and B4WWR (Figure 4.3, Figure 4.4, and Figure 4.5) are compared with a traditional reinforced beam B1RC (Figure 4.2) under a four point and uniformly distributed loading condition.

4.3.1 Rectangular Reinforced Concrete Beams Subjected to Four Point Loading Condition

For this analysis, a control beam B1RC is taken which is reinforced with conventional steel bars of 60,000 psi (415 MPa). The analysis results of this beam are compared with those from concrete beams B2WWR, B3WWR, and B4WWR with welded wires of 80,000 psi (550 MPa) and subjected to a four point bending test as shown in Figure 4.20. As explained earlier, a virtual experimental four point bending test is carried out in ABAQUS with the modeling

procedure being the same for all the beams. Their corresponding results have been explained later in this section.

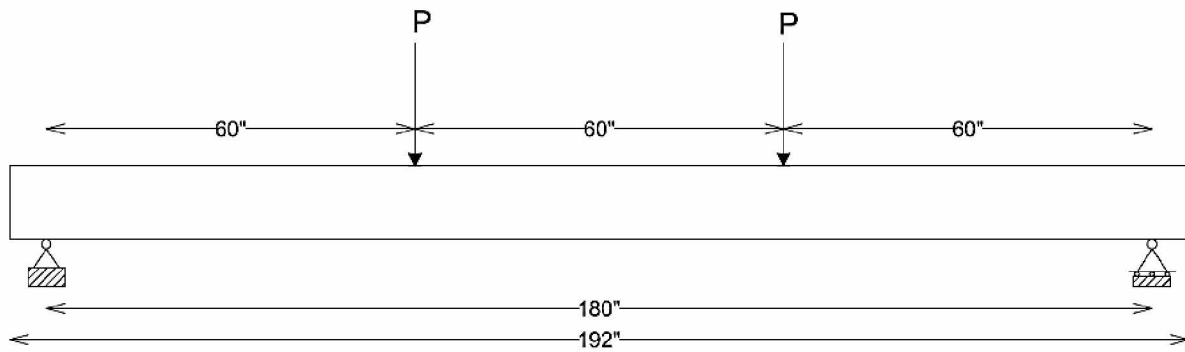


Figure 4.20: Four Point Bending Test Setup

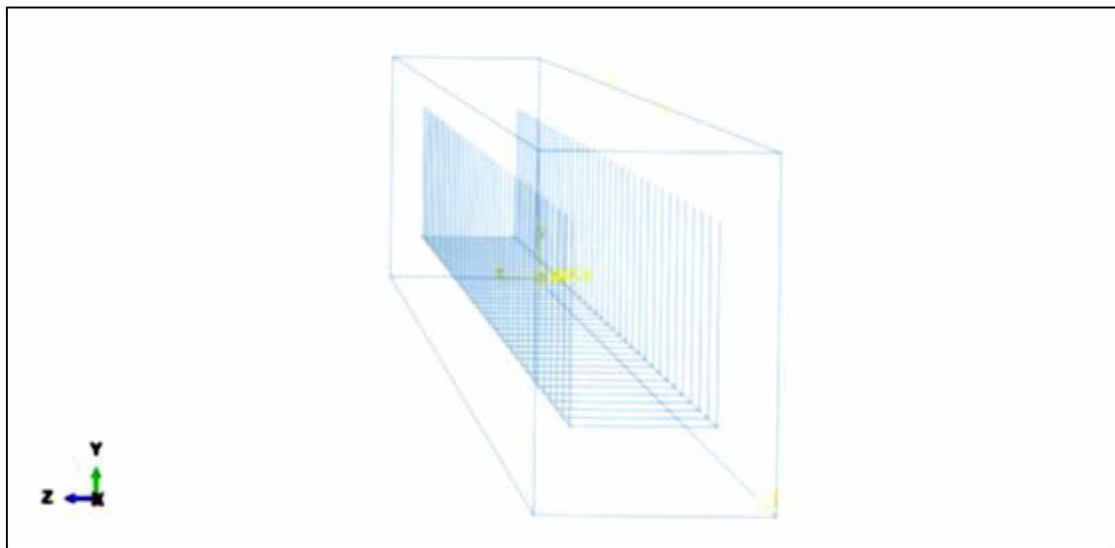


Figure 4.21: Open Leg Stirrup Embedded in B1RC Beam

Figure 4.21 shows control beam B1RC and its reinforcement embedment in the concrete beam, and Figure 4.22 shows the assembly of longitudinal and transverse wires and its embedment in concrete beam.

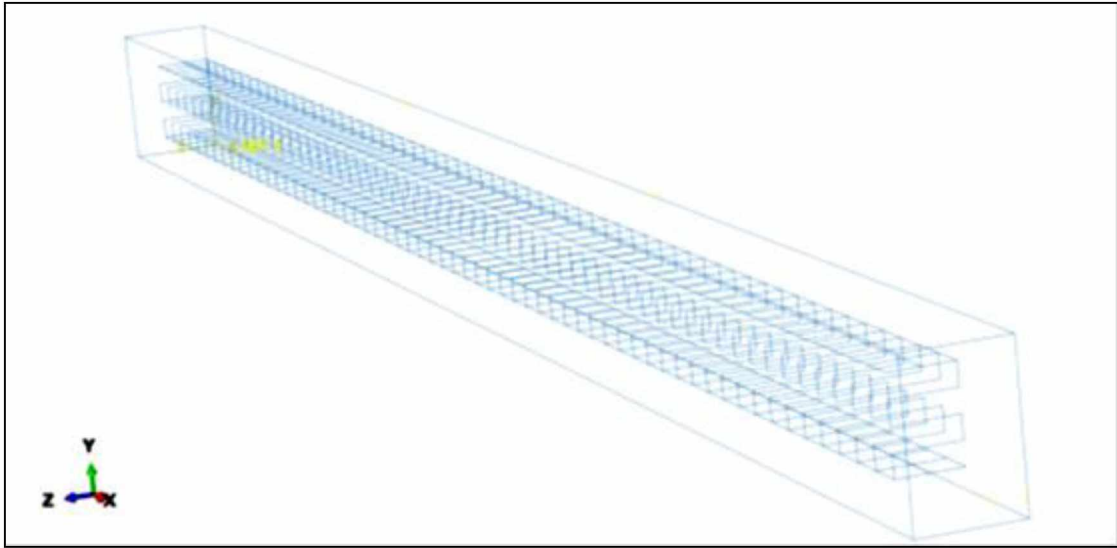


Figure 4.22: Welded Wire Reinforced B2WWR Beam

Figure 4.23 shows the embedment and load placement for four point bending test in B3WWR beam using reference points.

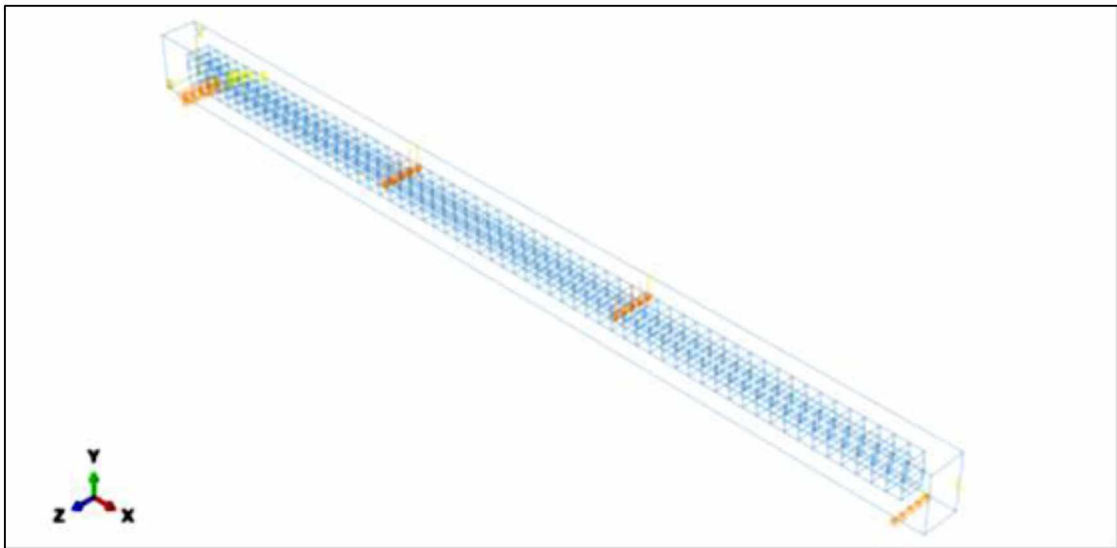


Figure 4.23: Virtual Four Point Bend Test Setup for the Beam

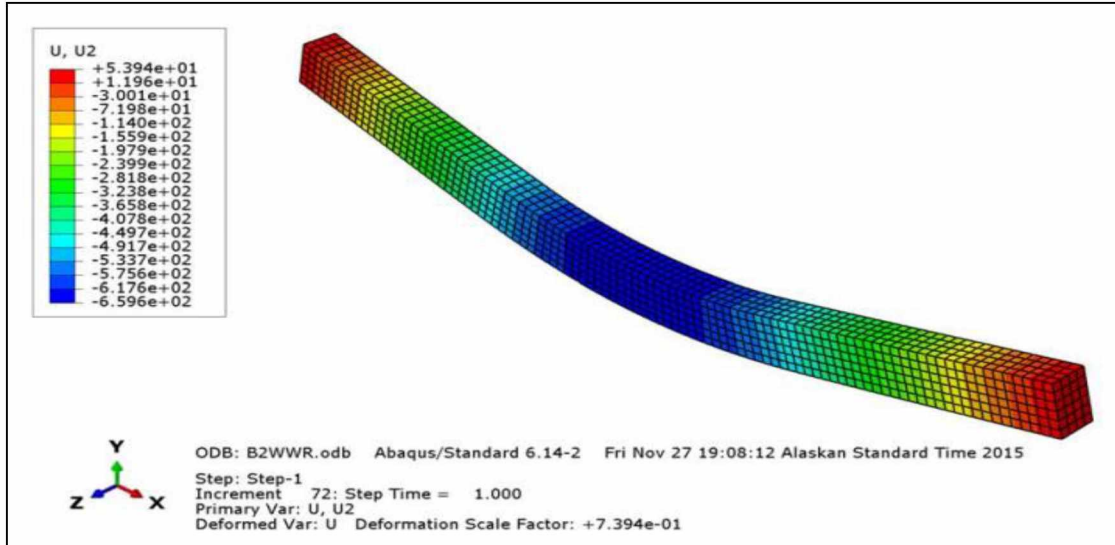


Figure 4.24: Deformed Behavior of B4WWR Beam after Analysis

Figure 4.24 shows the deformed shape of B4WWR beam. The load versus mid-span deflection graph for beams B1RC, B2WWR, B3WWR, and B4WWR are presented in Figure 4.25. Load versus mid-span deflection values have been extracted from the nodes that face the compressive side of the reinforced concrete beam. B4WWR beam being reinforced with 75% of flexural reinforcing of B1RC beam follows the same load versus deflection pattern as B1RC beam. As expected welded wire reinforced beams B2WWR and B3WWR follow the same pattern of load versus deflection. Being reinforced with 50% of flexural reinforcement, compared to B1RC beam, B2WWR and B3WWR have the same slope until a deflection of 0.2 inch (5 mm) and get declined with an increase in rate of deflection rate. At a particular deflection point of 1.2 inch (30.5 mm), the percentage difference between the load carrying capacity is minimal.

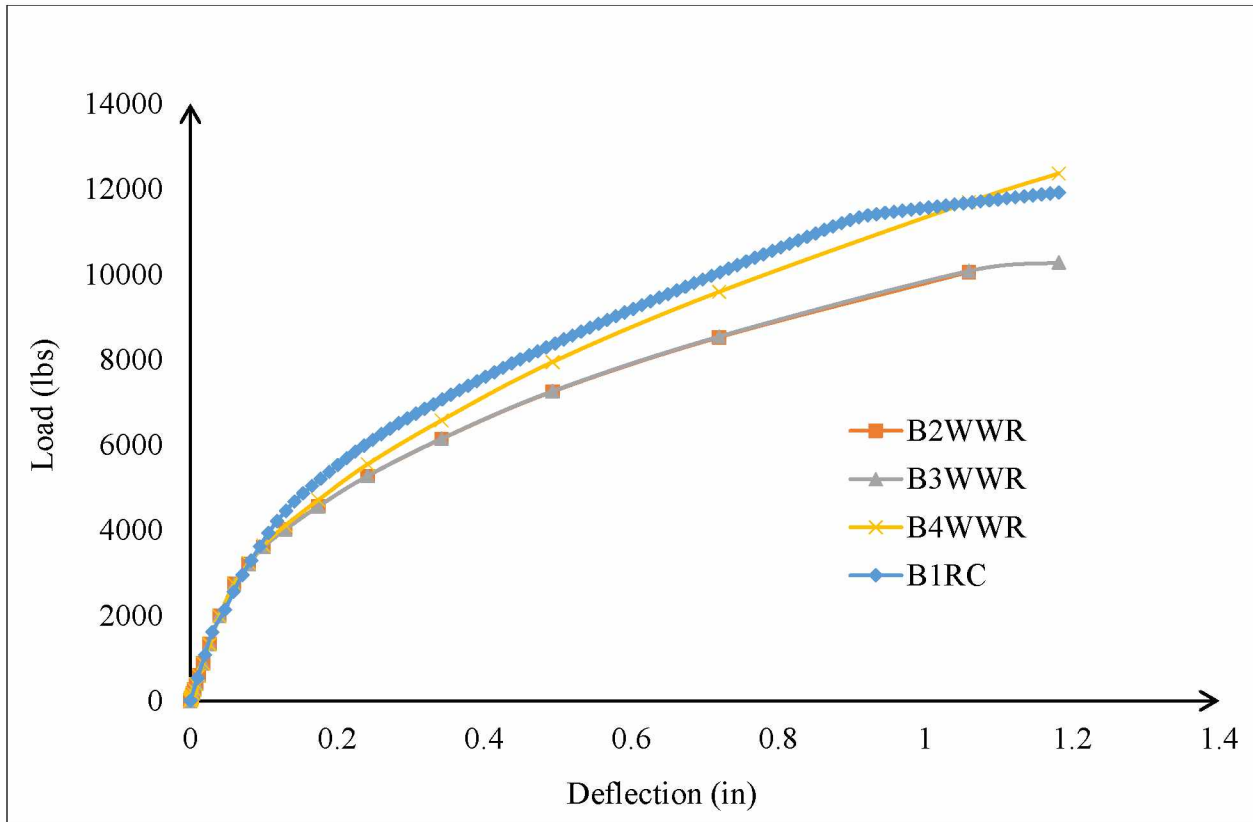


Figure 4.25: Load versus Deflection Graph for Rectangular Beams

Strain has been plotted along the length of the beam to understand the strain behavior of concrete and steel. A path has been created along the compressive face of the concrete and tension side of longitudinal steel to observe the strain behavior. Both concrete and steel strain values are plotted for beams B1RC, B2WWR, B3WWR, and B4WWR in Figure 4.26, Figure 4.27, Figure 4.28, and Figure 4.29.

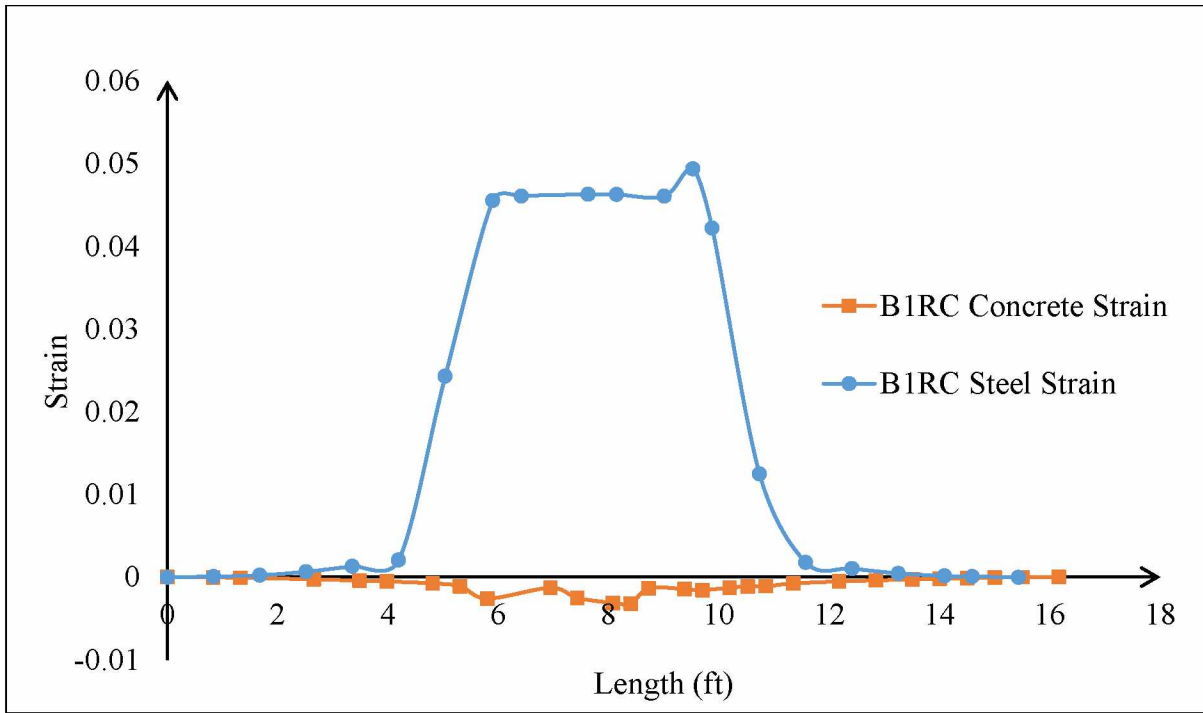


Figure 4.26: B1RC Concrete and Steel Strain along Length of Beam

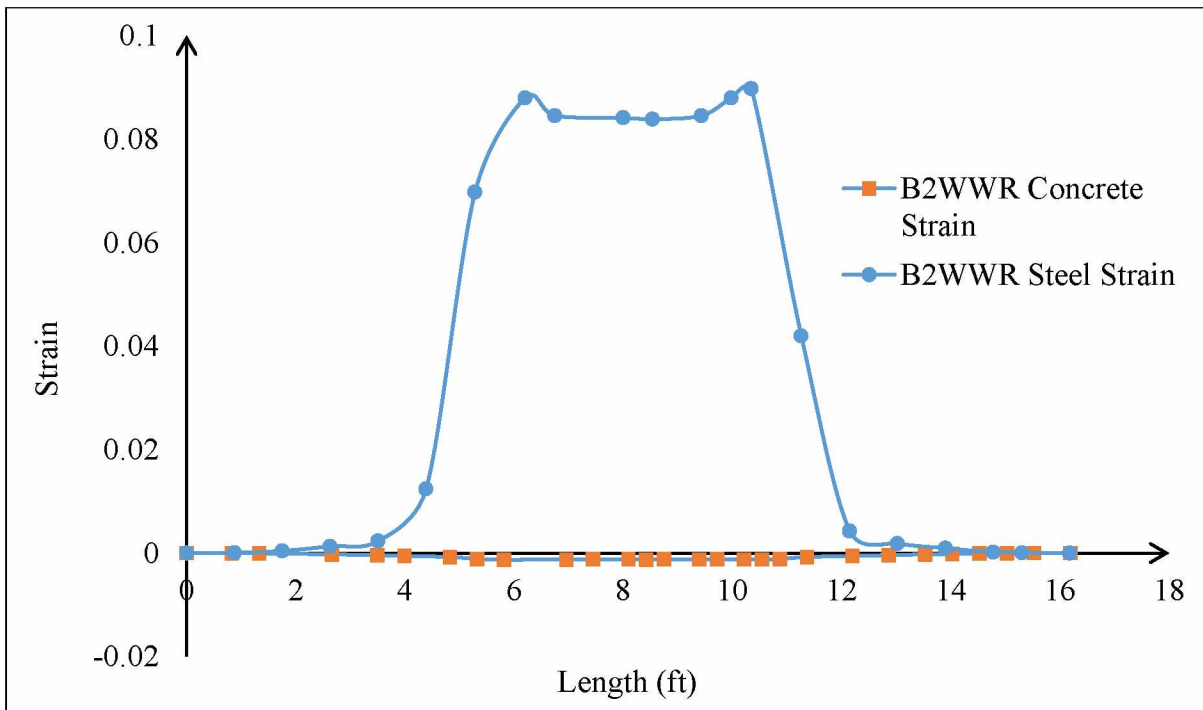


Figure 4.27: B2WWR Concrete and Steel Strain along Length of Beam

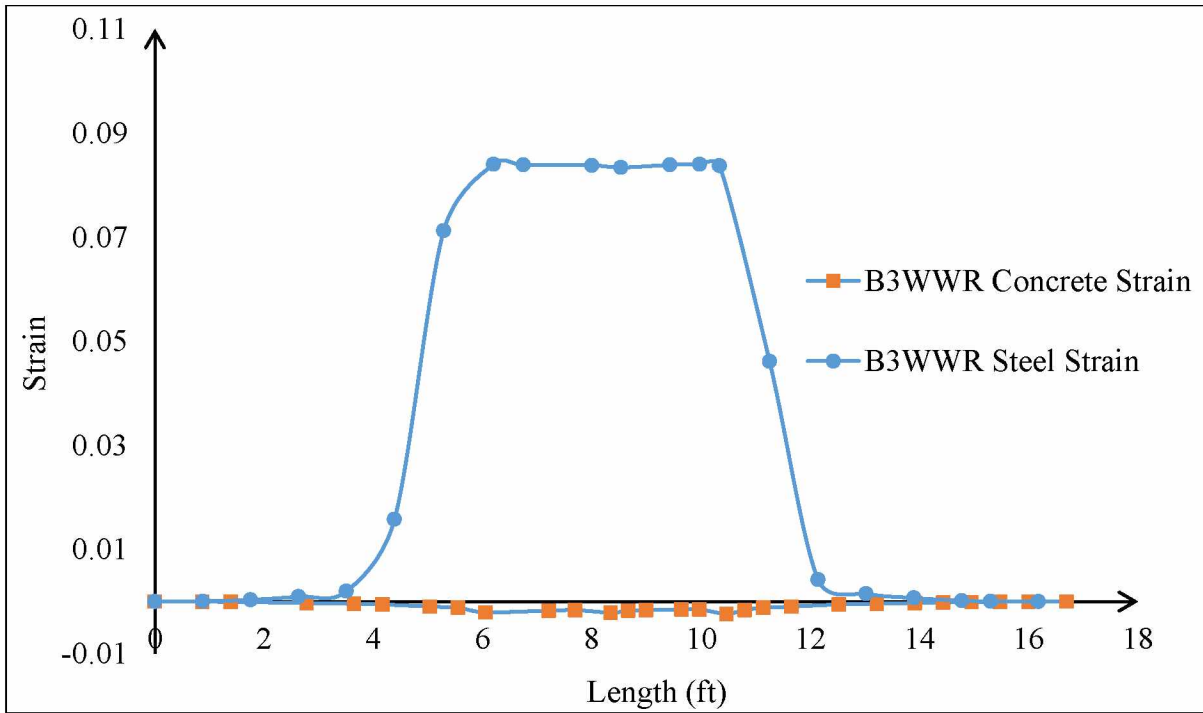


Figure 4.28: B3WWR Concrete and Steel Strain along Length of Beam

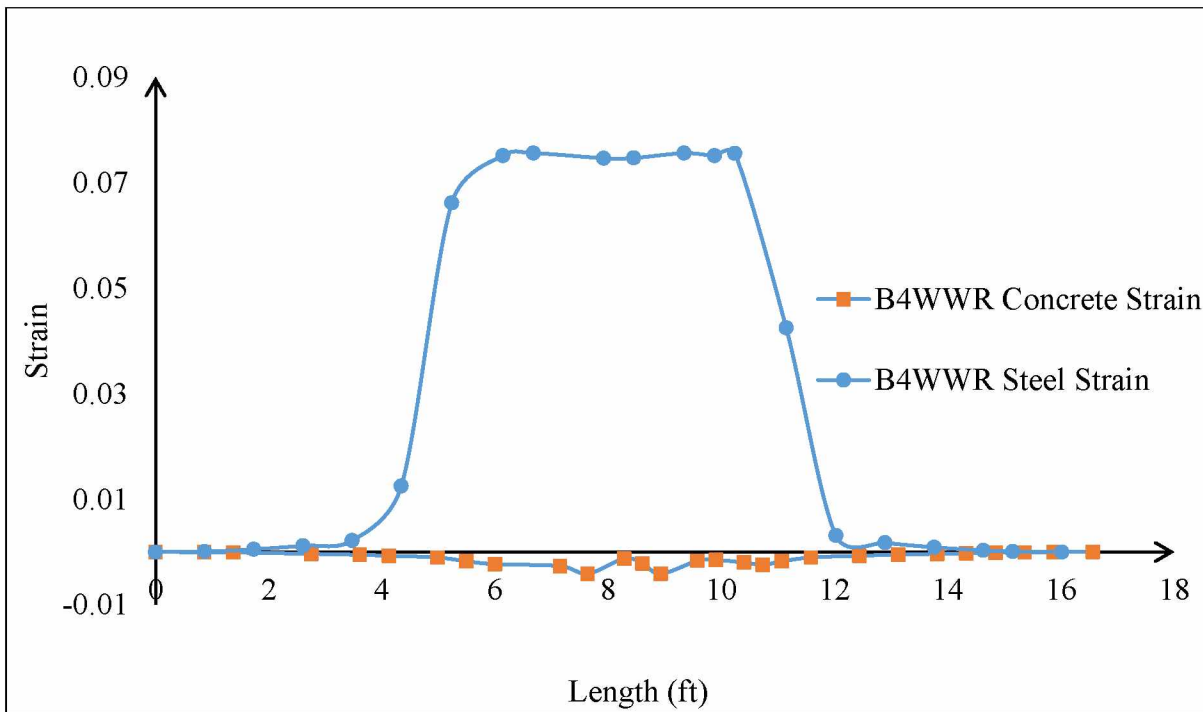


Figure 4.29: B4WWR Concrete and Steel Strain along Length of Beam

From Figure 4.26, Figure 4.27, Figure 4.28 and Figure 4.29 it is clear that the WWR beam can resist more strain than a beam reinforced with traditional reinforcement. Beam B1RC on the longitudinal steel has a maximum strain of 0.044 close to the mid span, but beams B2WWR, B3WWR, B4WWR have a strain value of 0.089, 0.084, 0.076 respectively.

Table 4.5: Moment and Shear Capacity for Beams under Four Point Loading Condition
* - Deflection for ϕP_n from Figure 4.25

Shape	Flexural Reinforcing Area (in ²)	F _y (Ksi)	ABAQUS		δ (in)*
			ϕM_n (Kip - ft)	ϕP_n (kip)	
B1RC	0.4	60	31.27	4.17	0.14
B2WWR	0.3	80	24.32	3.24	0.08
B3WWR	0.3	80	24.41	3.25	0.08
B4WWR	0.3	80	29.55	3.94	0.11

Using the ABAQUS feature view/cut manager module in the post processing window, beam moment capacity and shear capacity for the four point loading condition has been found when concrete strain reaches to 0.003, the nominal moment (ϕM_n) value is captured and tabulated in Table 4.5. Being reinforced with 75% of flexural reinforcing of B1RC beam, there is a 5.5% decrease in moment capacity between B4WWR and B1RC beam. Beams B2WWR and B3WWR carrying 50% of flexural reinforcing on the tension side have a 21.94% decrease in moment capacity when compared to B1RC beam. The ductility factor ($\Delta_{\text{maximum}}/\Delta_{\text{yield}}$) has been calculated from the load versus deflection graph (Figure 4.25) and tabulated here in Table 4.6.

Table 4.6: Ductility Factor for Beams under Four Point Loading Condition

Shape	Ductility Factor
B1RC	8.58
B2WWR	10
B3WWR	10
B4WWR	9.23

From Table 4.6, it is clear that stirrup which has a bent fashion and with half of its reinforcement of B1RC in tension side is more ductile than beams which have open (B1RC) and (B4WWR) closed rectangular stirrups. There is a ductility increase of 7.58% when the two beams B4WWR and B1RC are compared. A ductility increase of 16.55% is observed between B2WWR, B3WWR, and B1RC beams.

4.3.2 Rectangular Reinforced Concrete Beams Subjected to Uniformly Distributed Loading Condition

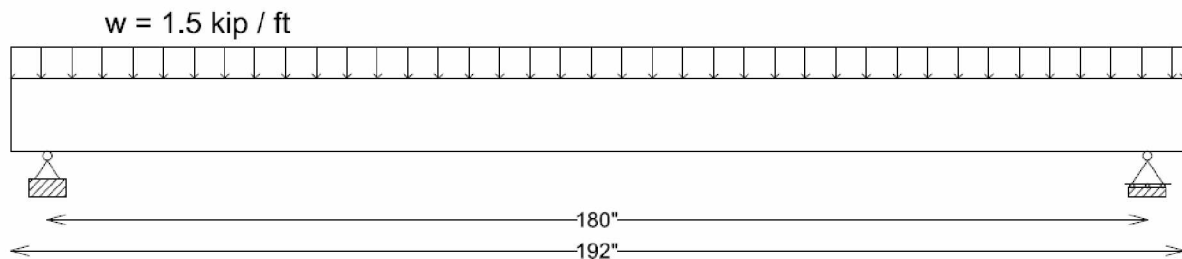


Figure 4.30: Uniformly Distributed Loaded Rectangular Beam

For this analysis, a control beam B1RC and three WWR beams (B2WWR, B3WWR, and B4WWR) are loaded by a uniformly distributed load (1.5 kip/ft) as shown in Figure 4.30.

As explained earlier, the modeling procedure is the same for all the beams and their corresponding results have been explained later in this section. Figure 4.31 shows the embedment and load placement for uniformly distributed load in B1RC beam.

The same loading condition has been adopted for beams B2WWR, B3WWR, and B4WWR and corresponding strain values have been observed along the length of the beam. Paths have been created along the compressive face of the concrete and the tension side of longitudinal steel to observe the strain behavior. Both concrete and steel strain have been plotted for all the rectangular beams and shown in Figure 4.32, Figure 4.33, Figure 4.34, and Figure 4.35.

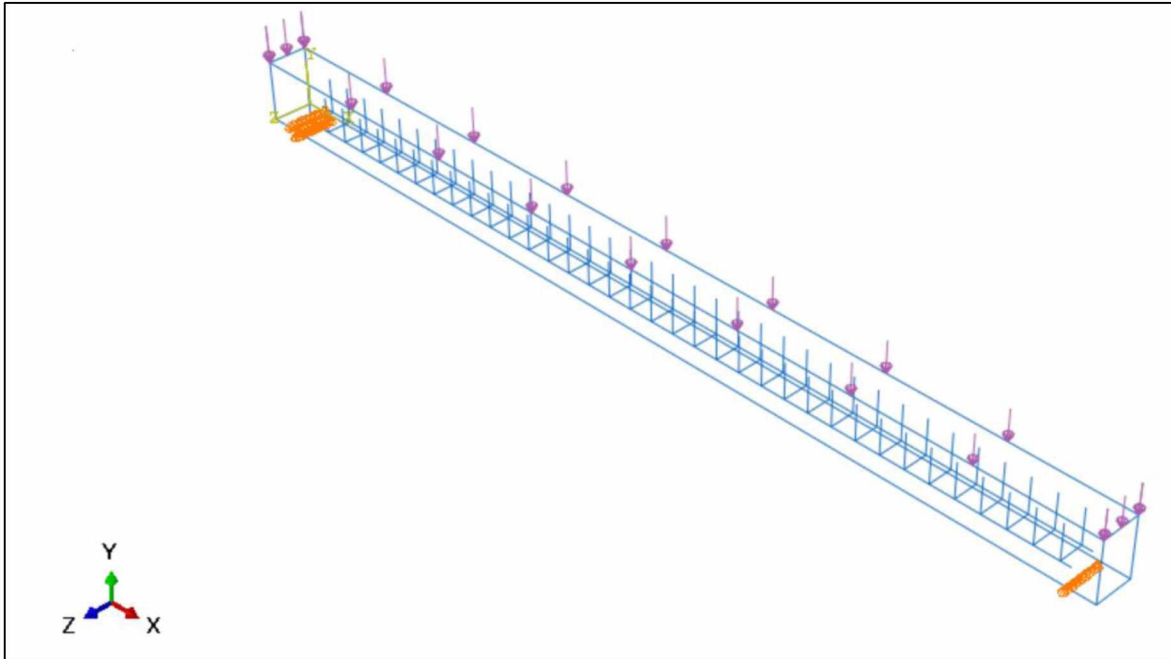


Figure 4.31: BIRC beam subjected to Uniformly Distributed Loading Condition

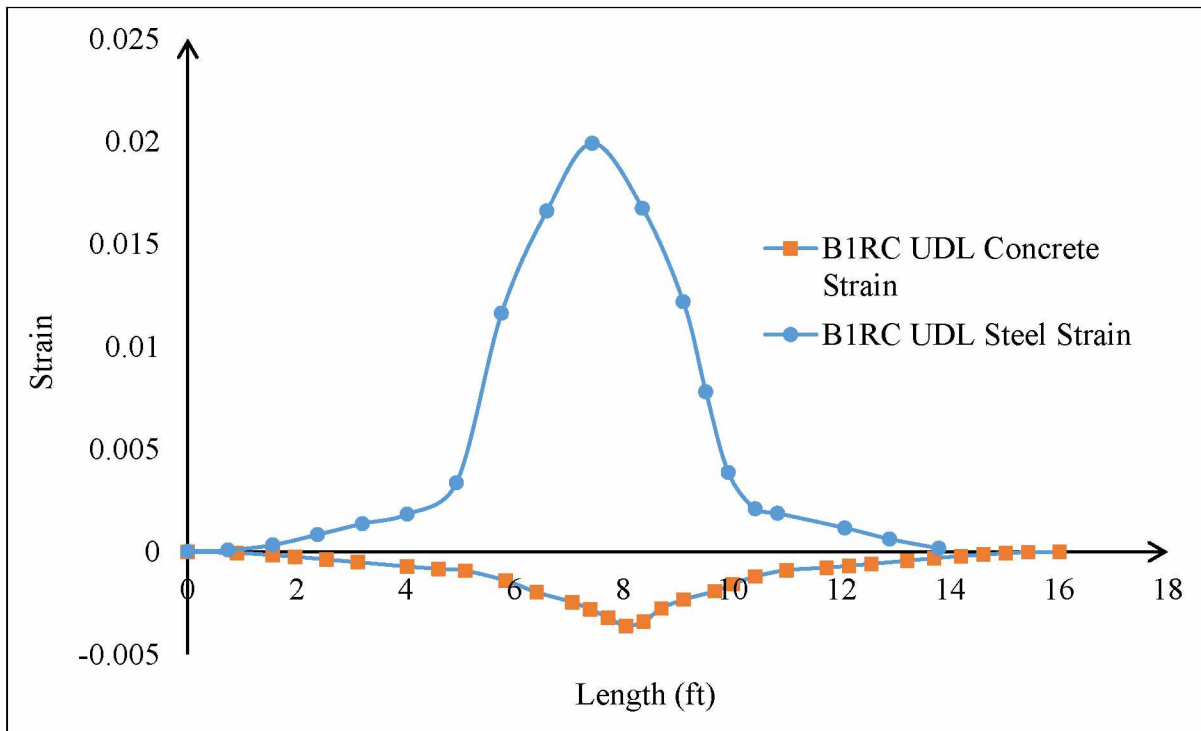


Figure 4.32: BIRC Concrete and Steel Strain along Length of Beam

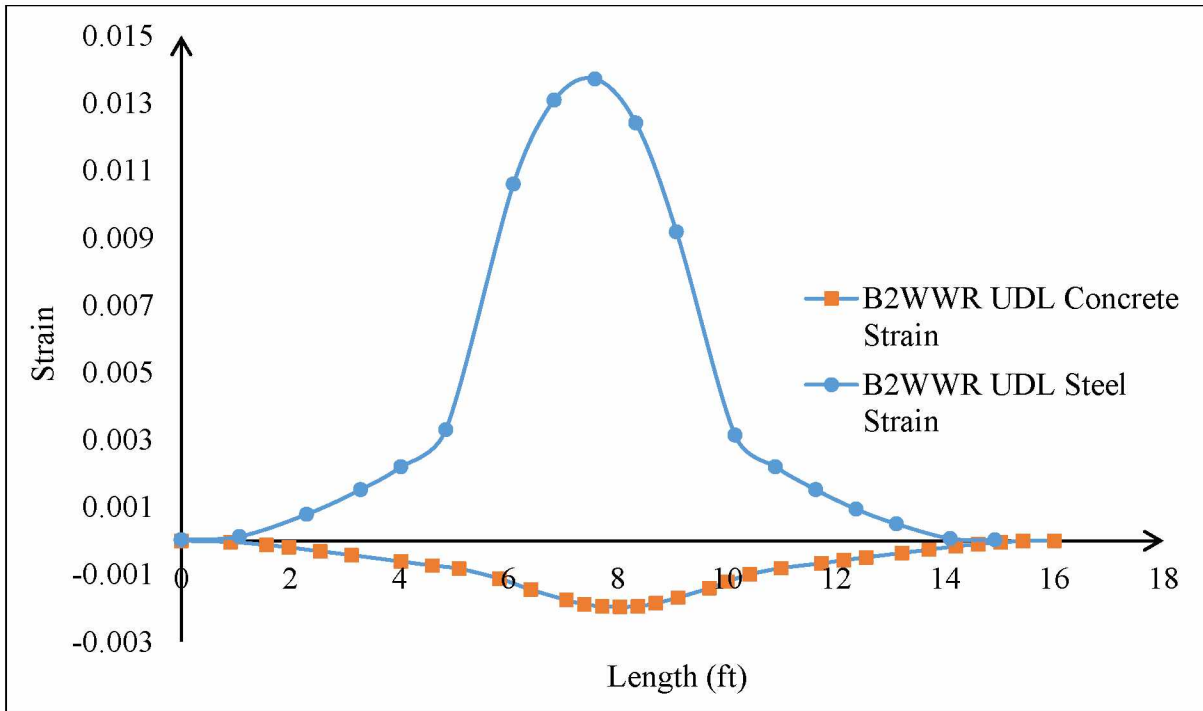


Figure 4.33: B2WWR Concrete and Steel Strain along Length of Beam

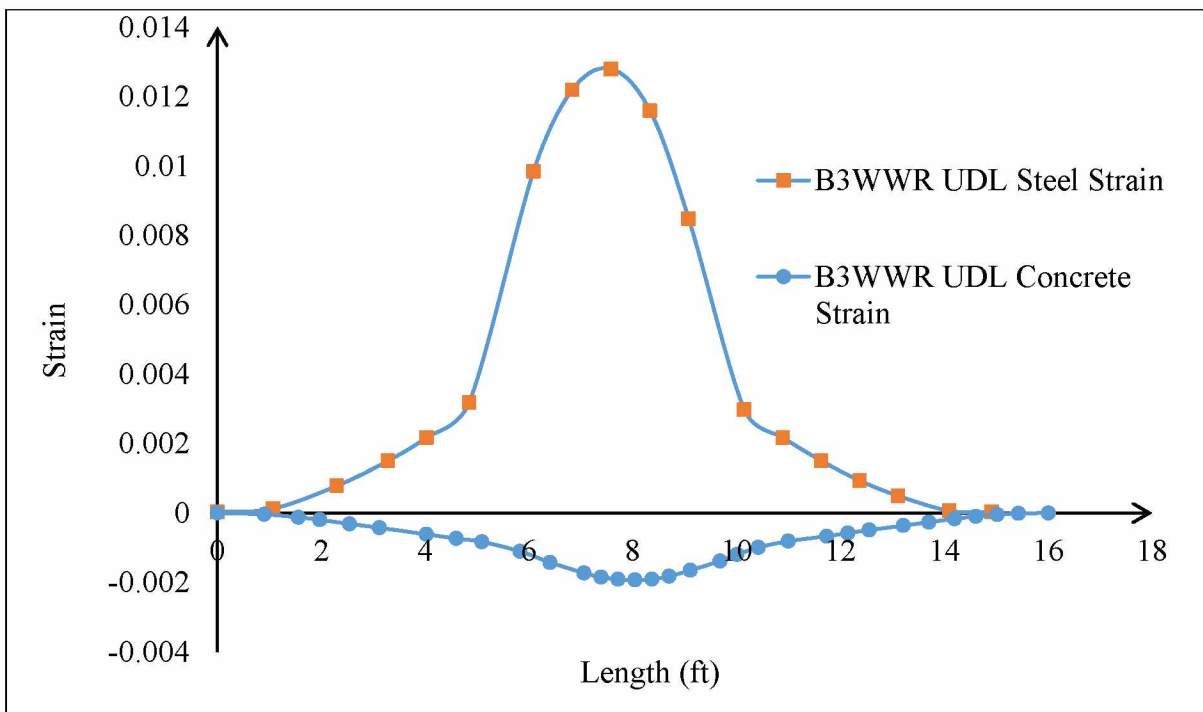


Figure 4.34: B3WWR Concrete and Steel Strain along Length of Beam

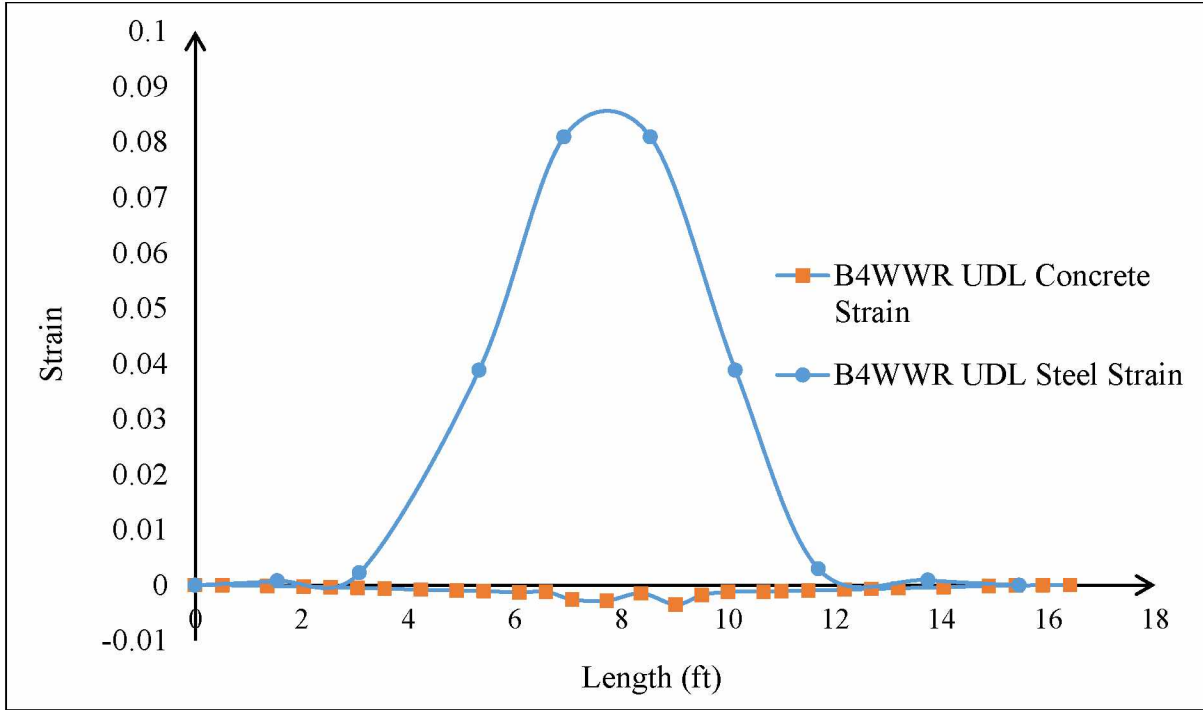


Figure 4.35: B4WWR Concrete and Steel Strain along Length of Beam

It is clear that the welded wire reinforced beam can resist more strain when compared to the beam reinforced with traditional reinforcement. Beam B1RC on the longitudinal steel has a maximum strain of 0.02 close to the mid span, but beams B2WWR, B3WWR, B4WWR have a strain value of 0.013, 0.013, and 0.08 respectively. Using the ABAQUS feature view/cut manager module in the post processing window, beam moment capacity and shear capacity for the four point loading condition have been found when concrete strain reaches to 0.003, the nominal moment (ϕM_n) and shear value (ϕV_n) is captured and tabulated in Table 4.7.

Table 4.7: Moment Capacity for Beams under Uniformly Distributed Loading Condition

Shape	Flexural Reinforcing Area (in ²)	Fy (ksi)	ϕM_n (kip - ft)	ϕV_n (kip)	ϕW_n (kip/ft)	Service load W.R.T L/360 deflection (kip)	Service load W.R.T L/240 deflection (kip)	Service load W.R.T L/180 deflection (kip)
B1RC	0.4	60	36.58	15.01	1.30	0.17	0.26	0.34
B2WWR	0.3	80	35.32	17.59	1.33	0.17	0.26	0.34
B3WWR	0.3	80	35.32	17.59	1.33	0.17	0.26	0.34
B4WWR	0.3	80	36.19	19.54	1.29	0.17	0.26	0.34

From Table 4.7, it is clear that the applied load (1.4 kip/ft) has been exactly extracted from the moment observed at the section where concrete strain reached 0.003. This proves that the reinforced concrete model is accurate enough to proceed to the second case of the study (T-beam reinforced concrete beam). Being reinforced with 75% of flexural reinforcing of B1RC beam, there is a 1.07% decrease in moment capacity and 30.18% increase in shear capacity between B4WWR and B1RC beams. Beams B2WWR and B3WWR carrying 50% of flexural reinforcing on the tension side has a 3.44% decrease in moment capacity and a 17.19% increase in shear capacity when compared to B1RC beam.

As it can be seen from the above discussion, both the control beam (B1RC) with conventional (60 ksi) reinforcement area of 0.4 in² (258 mm²) and the welded wire reinforced beam (B4WWR) of reinforcement area 0.3 in² (194 mm²) behave similarly in load and strain patterns. As expected WWR beams B2WWR and B3WWR have an identical response in load

and strain behavior. Based on the aforementioned comparison, welded wire reinforced beam B4WWR can be used as an alternative for the control beam B1RC.

4.3.3 T - Beams Subjected to Four Point Loading Condition

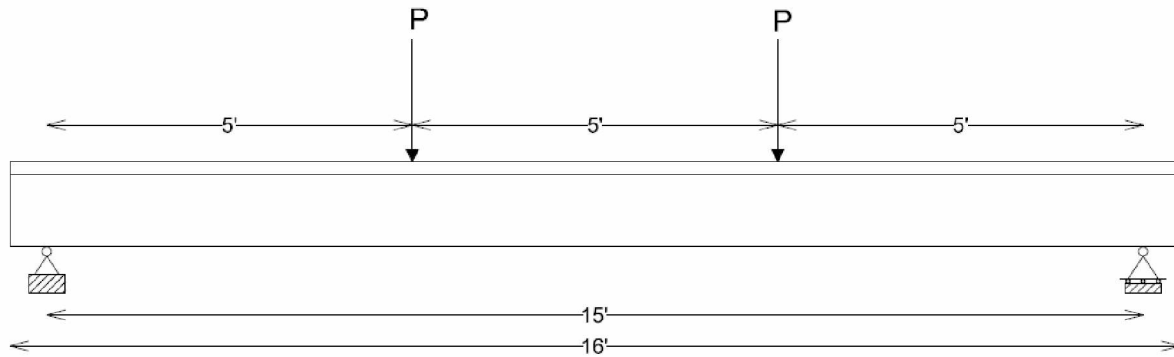


Figure 4.36: Four Point Bend Test Setup for T – Beam

For the second analysis case of the present study, Mexican chair styled reinforced grid TB1RC (Deacero 2015) is designed in accordance with B4WWR grid pattern using WWR of yield strength 80,000 psi (550 MPa) and subjected to a four point bend test as shown in Figure 4.36. Figure 4.37 and Figure 4.38 show the embeddement of Mexican chair styled reinforcement and WWR in T-beam.

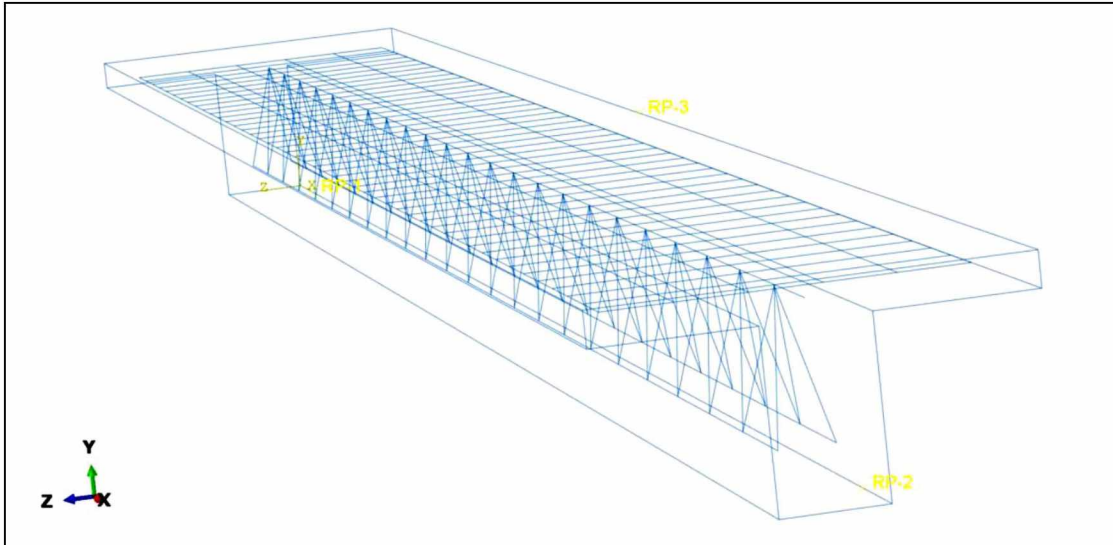


Figure 4.37: Mexican Chair Styled Reinforcement Embedded in T - Beam (TB1MS)

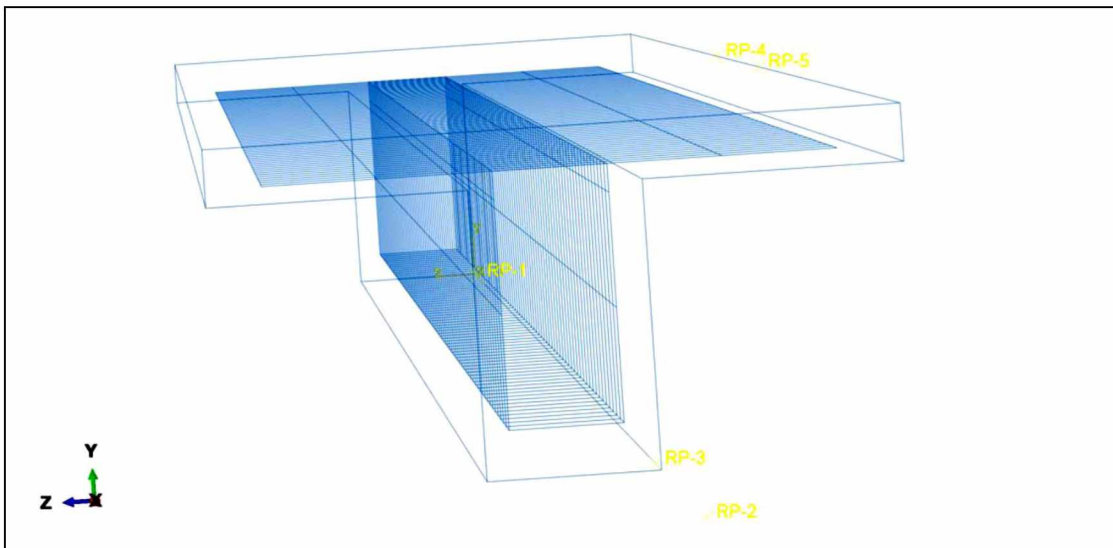


Figure 4.38: Welded Wire Mesh Embedded in T - Beam (TB2WWR)

Figure 4.40 shows the post processed analysis of four point bending test for a T-beam reinforced with WWR. The bending pattern is similar for both the beams TB1MS and TB2WWR.

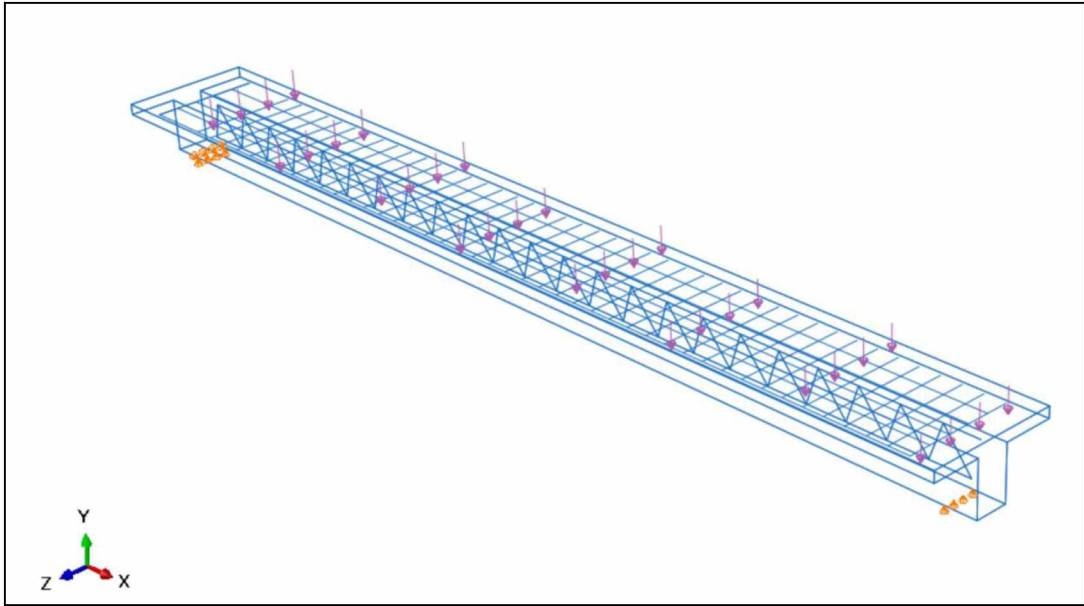


Figure 4.39: TB1RC beam subjected to Four Point Bend Test

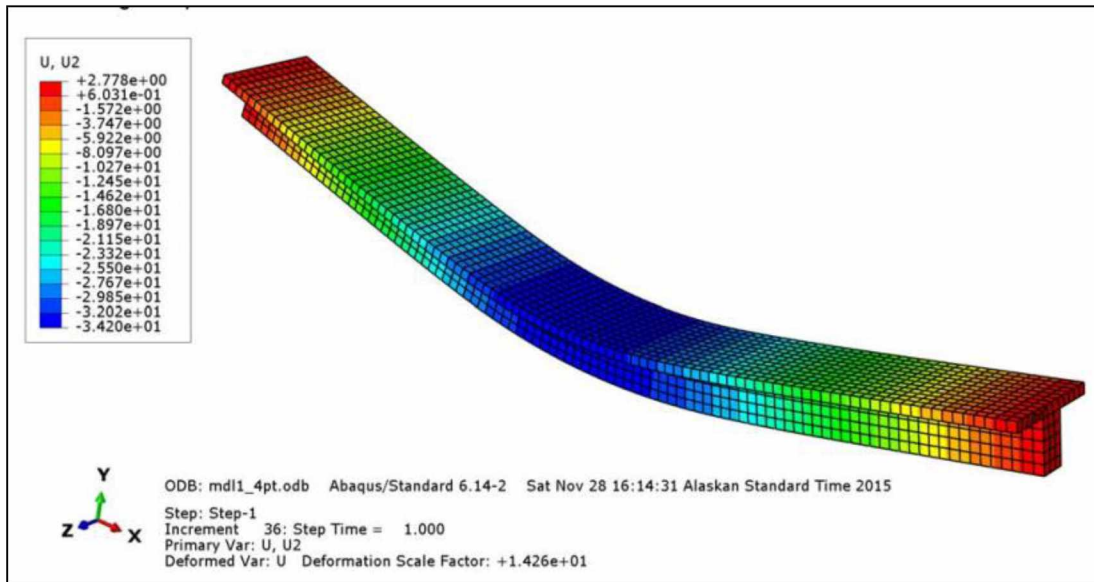


Figure 4.40: Deflected Shape of TB2WWR after Analysis

Figure 4.41 shows a load versus deflection relationship of T-beam for Mexican chair styled reinforcement pattern and WWR mesh. Load versus mid-span deflection values have been

extracted from the nodes that are on the compressive side of the reinforced concrete beam. TB2WWR beam being reinforced with 75% of flexural reinforcing of B1RC beam follows the same load versus deflection path as TB1MS beam. At a particular deflection point of 1.2 inch (30.5 mm), a 17.02% percentage increase in the load carrying capacity has been observed.

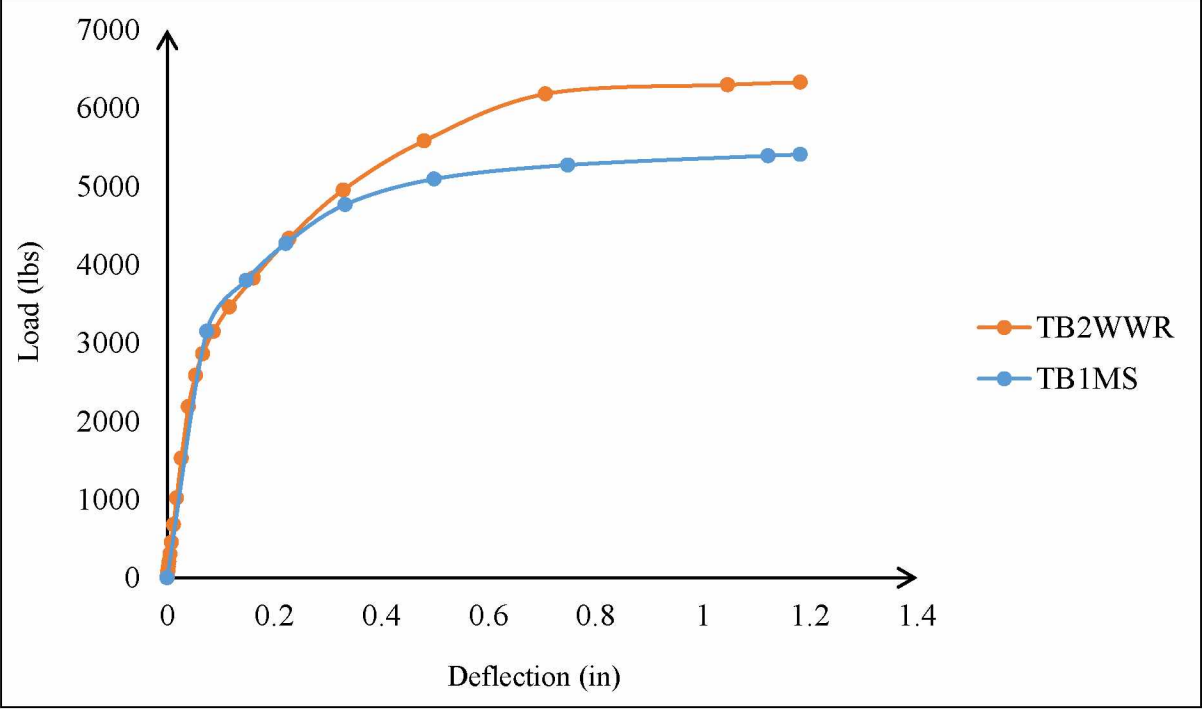


Figure 4.41: TB1MS, TB2WWR Load versus Deflection Graph

Table 4.8: Moment and Shear Capacity for T –Beam Subjected to Four Point Bending Test

* - Deflection for ϕP_n from Figure 4.41

Shape	Flexural Reinforcing Area (in ²)	F _y (ksi)	ABAQUS		δ (in)*
			ϕM_n (kip - ft)	ϕP_n (kip)	
TB1MS	0.4	60	14.86	1.98	0.01
TB2WWR	0.3	80	21.24	2.83	0.07

Using the ABAQUS feature view/cut manager module in the post processing window, beam nominal moment capacity (ϕM_n) for the four point loading condition has been extracted when concrete strain reaches to 0.003, and tabulated in Table 4.8. Being reinforced with 75% of flexural reinforcing of TB1MS beam, there is a 42.93% increase in nominal moment capacity (ϕM_n) between TB2WWR and TB1MS beam.

“This page intentionally left blank”

Chapter 5 Conclusion and Recommendation

5.1 Conclusion

The present study has been divided into two aspects: the effect of different types of reinforcement grids in rectangular beams and the effect of structurally performing grids in T-beams. For the first aspect, all the models with normal strength concrete (4500 psi), and the effect of different types of reinforcement grids (B1RC, B2WWR, B3WWR, and B4WWR) and strength (60 ksi and 80 ksi) has been evaluated. For the second aspect, T-beams have been subjected to a four point bending test. Concrete and steel properties are the same for all models subjected to the four point bending test and uniformly distributed loading.

From non-linear finite element analysis performed using ABAQUS, both the control beam (B1RC) with a conventional (60 ksi) reinforcement area of 0.4 in^2 (258 mm^2) and the WWR beam (B4WWR) with a reinforcement area of 0.3 in^2 (194 mm^2) behave similarly in load and strain patterns. The maximum strain in longitudinal steel of the B1RC beam was 0.044 close to the mid span, but maximum strain values for the B2WWR, B3WWR, and B4WWR beams were 0.089, 0.084, and 0.076, respectively. When subjected to a four point bending test, there was a 5.5% decrease in moment capacity between the B4WWR and B1RC beams. The ductility of the B4WWR beam increased by 7.58% when compared to the B1RC beam. When a rectangular reinforced concrete beam is subjected to a uniformly distributed load of 1.5 kip/ft, there is a 1.07% decrease in moment capacity and a 30.18% increase in shear capacity between the B4WWR and B1RC beams. Based on the aforementioned comparison, a welded wire reinforced B4WWR beam can be used as an alternative for the control B1RC beam.

WWR beams B2WWR and B3WWR follow the same pattern of load versus deflection behavior, but being reinforced with 50% of the flexural reinforcement, at a particular deflection

point of 1.2 inch (30.5 mm), the percentage difference in the load carrying capacity between the two beams is minimal. B2WWR and B3WWR have a 21.94% decrease in moment capacity when they were compared to B1RC beam. The ductility increase was 16.55% between B2WWR, B3WWR and B1RC when subjected to a four point bending test. B2WWR and B3WWR carrying 50% of flexural reinforcing on the tension side have a 3.44% decrease in moment capacity and a 17.19% increase in shear capacity when compared to B1RC beam subjected to a uniformly distributed load. Based on the aforementioned comparison, WWR beam B4WWR can be used as an alternative for the control beam B1RC.

Being reinforced with 75% of flexural reinforcing of TB1MS beam, there is a 42.93% increase in moment capacity between TB2WWR and TB1MS beams.

According to the results of the present study, it can be concluded that WWR (80,000 psi) can be a better alternative over traditional reinforcing bars (60,000 psi). Welded wire reinforcement grids have a highest flexural capacity with less reinforcing area and with smaller diameter bars, which enhances load transfer mechanism.

5.2 Recommendation

The following investigations are recommended.

- Numerical analysis of welded wire reinforced beams B2WWR, B3WWR, B4WWR, and TB2WWR have to be validated through experimental means.
- The effective part of improving the study can be done by studying the stress and strain properties of welded wires by the tensile test method.
- T-beam reinforced with welded wires subjected to a uniformly distributed load has to be modeled in ABAQUS and its performance has to be observed carefully.

- Furthermore research has to be done on rehabilitation of structural components with welded wire mesh.
- More research has to be conducted on improving the automation techniques which improves the accessibility of WWR.

“This page intentionally left blank”

References

- American Concrete Institute. 2011. "Building Code Requirements for Structural Concrete and Commentary (ACI 318 – 11)".
- American Society for Testing and Materials. 2003. "Specification for Welded Wire Reinforcement". www.astm.org
- Arbeitszeitwerte Fuer Das Verlegen. 1977.
<http://rebar.ecn.purdue.edu/wwr/Library%5CPotential%20Gains>
- Bernold, L., and Chang, P. 1992. "Potential gains through welded wire reinforcement". *Journal of Construction Engineering and Management*.
- Chen A. T. C, and Chen W. F. 1975. "Constitutive Relations for Concrete". *Journal of Engineering Mechanics, ASCE*, V. 101, No. 4: 465 – 481.
<http://cedb.asce.org/cgi/WWWdisplay>
- Chong K. T. 2004. "Numerical Modeling of Time-dependent Cracking and Deformation of Reinforced Concrete Structures". Doctoral Thesis, University of New South Wales, Sydney, Australia, December 2004.
- Deacero – Steel and Welded Wire Reinforcements. 2015.
<http://www.deacero.com/us/products.html>
- Durrani, A., and Robertson, I. 1987. "Shear Strength of Prestressed Concrete T-Beams with Welded Wire Fabric as Shear Reinforcement". *PCI Journal*: 46 – 61.
http://www.pci.org/pci_journal-1987-march-april-4/
- Feensta P. H, and De Borst R. 1996. "A composite plasticity model for concrete". *International journal of Solid Structures*, V. 33, No. 5: 707 - 730.
<http://www.researchgate.net/publication/27343687>

- Gopinath, S., Murthy, R., Iyer, N., and Prabha, M. 2014. "Behavior of Reinforced Concrete Beams Strengthened With Basalt Textile Reinforced Concrete". *Journal of Industrial Textiles*. <http://jit.sagepub.com/content/early/2014/01/30/1528083714521068>
- Han D. J, and Chen W. F. 1985. "A non-uniform hardening plasticity model for concrete materials". *Mechanics of Materials*, V. 4: 283 – 302.
- Hibbitt, D., Karlsson, B., and Sorensen, P. 2013. ABAQUS Documentation, Dassault Systems 2013. <http://129.97.46.200:2080/v6.13/>
- Jankowaik, T., and Lodygowski, T. 2006. "Identification of Parameters of Concrete Damage Plasticity Constitutive Model". *Foundations of Civil and Environmental Engineering*, V. 6: 53 – 69.
- Johnson, D. 1969. "Partial Interactive Design of Composite Beam". *International Journal of Composite and Structures*, V. 53: 305 – 311.
- Kaufmann W. 1988. "Strength and Deformations of Structural Concrete Subjected to In-Plane Shear and Normal Forces". Doctoral Thesis, Swiss Federal Institute of Technology, Zurich, Switzerland, 1988.
- Kupfer H., and Gerstle K. H. 1973. "Behavior of Concrete under Biaxial Stresses". *Journal of the Engineering Mechanics Division, ASCE*, V. 99: 552 – 866.
<http://cedb.asce.org/cgi/WWWdisplay>
- Kusuma, B., Tavio, S., and Suprobo, P. 2015. "Behavior of Concentric Loaded Welded Wire Fabric Reinforced Concrete Columns with Varying Reinforced Grids and Ratios". *International Journal of ICT – aided Architecture and Civil Engineering*, Vol. 2, No. 1: 1 – 14. http://www.sersc.org/journals/IJIACE/vol2_no1/1

- Mansur M. A, Lee C. K, and Lee S. L. 1988. “Deformed Wire Fabric as Shear Reinforcement in Concrete Beams”. *ACI Structural Journal*: 392 - 399.
- Morcous, G., Maguire, M., and Tadros, M. 2011. “Welded Wire Reinforcement versus random Steel Fibres in Precast, Pre-stressed Concrete Girders”. *Precast/Pre-stressed Concrete Institute*: 113-129.
- Purdue – Welded Wire Reinforcement. 2015.
<http://rebar.ecn.purdue.edu/wwr/resDesign.aspx>
- Reiterman, R. 1992. “Welded Wire Reinforcement for Columns”. *ACI Structural Journal*: 473 – 474.
- Razvi, S., and Saatcioglu, M. 1989. “Confinement of Reinforced Concrete Columns with Welded Wire Fabric”. *ACI Structural Journal*, V. 86, No. 5: 615 – 623.
- Riva, P., and Franchi, A. 2001. “Behavior of Reinforced Concrete Walls with Welded Wire Mesh subjected to Cyclic Loading”. *ACI Structural Journal*, V. 98, No. 3: 324 – 334.
- Schnell Reinforcement Processing Equipment. 2015.
<http://www.schnell.it/?lang=en>
- Wire Reinforcement Institute – Manual of Standard Practice. 2006.
<http://www.cwri.com/Manual%20of%20Standard%20Practice>
- Welded Wire Mesh. 2012.
https://www.welded+wire+mesh&rlz=1C1CHWA_enUS629US629&source=lnms&tbn
- Xuan, X., Rizkalla, S., and Maruyama, K. 1987. “Effectiveness of Welded Wire Fabric as Shear Reinforcement in Pretensioned Prestressed Concrete T-Beams”. *ACI structural Journal*: 429 – 436.